Quantum Electronics **32** (5) 377–400 (2002) ©2002 Kvantovaya Elektronika and Turpion Ltd

REVIEW

PACS numbers: 42.25.Bs; 42.25.Gy
DOI: 10.1070/QE2001v031n05ABEH002205

Whispering-gallery waves

A.N. Oraevsky

Contents

***Abstract*. A review of the theory of the natural waves (eigenmodes) in a dielectric sphere is presented. A special attention is paid to the eigenmodes with large radial and azimuthal indices, the so-called whispering-gallery modes. The experimental results of the spectroscopic study of modes in a dielectric sphere are reported. The fields of applications of whispering-gallery modes are discussed.**

Keywords: *Debye potentials, dielectric-sphere modes, whispering-gallery modes, resonance frequencies, mode Q-factor.*

1. Introduction

In Peking, near a famous historical memorial, the Temple of Sky, there is a miraculous stone wall, which forms an almost closed cylinder. The 'miracle' consists in the fact that sounds uttered in a low voice in one of the directions along the wall return back after some time to a person who uttered them. It seems that somebody invisible behind the back of the person pronounce the same sounds by the person's voice.

The modern physical explanation of this effect was proposed by Rayleigh as early as over a century ago [1]. Rayleigh explained the effect on the basis of his own observations made in an ancient gallery located under the dome of St. Paul's Cathedral in London (Fig. 1). This gave the name *whispering-gallery waves* for these waves. Before Rayleigh, this effect was assigned to the reflection of acoustic 'rays' from a surface near the dome apex. It was assumed that the rays propagated along different large arcs of the dome in the form of a hemisphere should concentrate only at the point that is located diametrically opposite to a sound source. However, Rayleigh found that, along with this effect, another effect exists: sound 'clutches' to the wall surface and 'creeps' along it. The concave surface of the dome does not allow the beam cross section to expand as fast as during propagation in free space. While in the latter case the beam cross section increases and the radiation intensity decreases proportionally to the square of distance from a source, the radiation in the whispering gallery propagates within a narrow layer adjacent to the wall surface. As a result, the sound intensity inside this layer decreases only directly proportionally to the distance, i.e., much slower than in free space. Rayleigh confirmed his explanation by direct experiments using a whistle as a sound source and a burning candle as a detector.

It was found much later, at the beginning of the 20th

A.N. Oraevsky P.N. Lebedev Physics Institute, Russian Academy of Sciences, Leninskii prosp. 53, 119991 Moscow, Russia;
e-mail: oraevsky@maill.lebedev.ru

Received 23 January 2002
Kvantovaya Elektronika **32** (5) 377–400 (2002)
Translated by M.N. Sapozhnikov

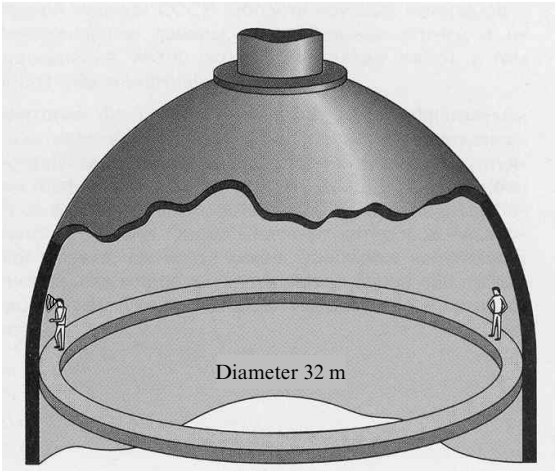

Figure 1. Whispering gallery under the dome of St. Paul's Cathedral in London.

century [2–4], that in dielectric spheres the electromagnetic waves can exist, which have the same spatial structure as whispering-gallery acoustic waves. The waves of this type did not attract much attention until the last decade when they suddenly became the objects of wide studies and applications in optics. Why?

To answer this question, it is necessary to understand what the whispering-gallery waves are and under what conditions they can appear. This requires the study of the structure of fields in dielectrics. Below, we consider the electrodynamics of a dielectric sphere. The electrodynamics of dielectric cylinders, dielectric spherical layers, and aspherical bodies remains beyond the scope of this review. The electrodynamics of a dielectric cylinder provides the basis for the theory of dielectric fibres and is described in monographs (see, for example, [5]). As for the electrodynamics of dielectric spherical layers and aspherical bodies, it is appropriate to consider these problems in a special review.

2. Basic equations. Debye potentials

Before studying the waves in a dielectric sphere, we will show, following book [6], that the solution of Maxwell's equations for space with a dielectric sphere can be reduced to the solution of a scalar equation for the so-called Debye potentials [3].

Maxwell's equations for a monochromatic field

$$\operatorname{rot} \boldsymbol{E} = \mathrm{i}k\boldsymbol{H}, \ \operatorname{rot} \boldsymbol{H} = -\mathrm{i}k\boldsymbol{E} \tag{1}$$

in the curvilinear coordinate system ξ_1, ξ_2, ξ_3 have the form

$$\frac{\partial}{\partial \xi_n}\left(L_m E_m\right) - \frac{\partial}{\partial \xi_m}\left(L_n E_n\right) = \mathrm{i}k L_m L_n H_l, \tag{2a}$$

$$\frac{\partial}{\partial \xi_n}\left(L_m H_m\right) - \frac{\partial}{\partial \xi_m}\left(L_n H_n\right) = -\mathrm{i}k L_m L_n E_l, \tag{2b}$$

where $k = (\omega/c)(\varepsilon\mu)^{1/2}$; ε and μ are the dielectric constant and magnetic permeability of the sphere; L_1, L_2, L_3 are Lame's coefficients; $m = 1, 2, 3, n = 1, 2, 3,$ and $l = 1, 2, 3,$ and $m \neq n \neq l$. Upon substituting the specific values of $m, n,$ and l in Eqns (2), the circular sequence 321, 132, 213 of the indices should be fulfilled. If this sequence is violated, the sign of the right-hand side of Eqns (2) should be changed to opposite.

The solution of the system of equations (2) involves the obtaining of six scalar functions representing the six projections of the vectors of the electric and magnetic fields. However, for certain relations between Lame's constants, electromagnetic fields can be divided into two subgroups: the subgroup of waves of the electric type and the subgroup of waves of the magnetic type.

For the waves of the electric type (E type), one of the components of the magnetic field (for example, H_3) is identically zero, whereas all other components are nonzero, generally speaking. For the waves of the magnetic type, one of the components of the electric field (for example, E_3) is identically zero, whereas all other components are nonzero, generally speaking. In this case, each of the subgroups can be defined with the help of one scalar function. Let us show it.

Consider waves of the E type ($H_3 = 0$). It follows from Eqn (2a) for $l = 3$ that

$$\frac{\partial}{\partial \xi_1}\left(L_2 E_2\right) = \frac{\partial}{\partial \xi_2}\left(L_1 E_1\right). \tag{3}$$

After the introduction of the function W such that

$$L_1 E_1 = \frac{\partial W}{\partial \xi_1}, \quad L_2 E_2 = \frac{\partial W}{\partial \xi_2}, \tag{4}$$

Eqn (3) is satisfied identically. By substituting relation (4) into Eqns (2b) corresponding to indices $l = 1, 2$, we find

$$\frac{\partial}{\partial \xi_3}\left(L_2 H_2\right) = \mathrm{i}k \frac{L_2 L_3}{L_1} \frac{\partial W}{\partial \xi_1}, \tag{5a}$$

$$\frac{\partial}{\partial \xi_3}\left(L_1 H_1\right) = -\mathrm{i}k \frac{L_1 L_3}{L_2} \frac{\partial W}{\partial \xi_2}. \tag{5b}$$

Let us assume now that $L_3 = 1$ and the ratio L_1/L_2 is independent of ξ_3. Then, assuming that $W = \partial U/\partial \xi_3$, where U is an unknown function yet, we find

$$H_1 = -\mathrm{i}k \frac{1}{L_2} \frac{\partial U}{\partial \xi_2}, \ H_2 = \mathrm{i}k \frac{1}{L_1} \frac{\partial U}{\partial \xi_1}. \tag{6}$$

In this case, according to Eqn (2b), E_3 is determined by the relation

$$E_3 = -\frac{1}{L_1 L_2}\left[\frac{\partial}{\partial \xi_1}\left(\frac{L_2}{L_1}\frac{\partial U}{\partial \xi_1}\right) + \frac{\partial}{\partial \xi_2}\left(\frac{L_1}{L_2}\frac{\partial U}{\partial \xi_2}\right)\right]. \tag{7}$$

Therefore, all the components of the electromagnetic field are expressed in terms of one scalar function U. It is necessary to find to what equation this function satisfies. We have at our disposal two equations of system (2):

$$\frac{\partial}{\partial \xi_2}\left(L_3 E_3\right) - \frac{\partial}{\partial \xi_3}\left(L_2 E_2\right) = \mathrm{i}k L_2 L_3 H_1, \tag{8a}$$

$$\frac{\partial}{\partial \xi_3}\left(L_1 E_1\right) - \frac{\partial}{\partial \xi_1}\left(L_3 E_3\right) = \mathrm{i}k L_3 L_1 H_2. \tag{8b}$$

By substituting expressions (6) and (7) into Eqns (8), we obtain

$$\frac{\partial}{\partial\xi_1}\left\{\frac{\partial^2 U}{\partial\xi_3^2}+\frac{1}{L_1L_2}\left[\frac{\partial}{\partial\xi_1}\left(\frac{L_2}{L_1}\frac{\partial U}{\partial\xi_1}\right)+\frac{\partial}{\partial\xi_2}\left(\frac{L_1}{L_2}\frac{\partial U}{\partial\xi_2}\right)\right]+k^2U\right\}=0, \tag{9a}$$

$$\frac{\partial}{\partial\xi_2}\left\{\frac{\partial^2 U}{\partial\xi_3^2}+\frac{1}{L_1L_2}\left[\frac{\partial}{\partial\xi_1}\left(\frac{L_2}{L_1}\frac{\partial U}{\partial\xi_1}\right)+\frac{\partial}{\partial\xi_2}\left(\frac{L_1}{L_2}\frac{\partial U}{\partial\xi_2}\right)\right]+k^2U\right\}=0. \tag{9b}$$

Both these equations are satisfied simultaneously if the function U is the solution of the equation

$$\frac{\partial^2 U}{\partial\xi_3}+\frac{1}{L_1L_2}\left[\frac{\partial}{\partial\xi_1}\left(\frac{L_2}{L_1}\frac{\partial U}{\partial\xi_1}\right)+\frac{\partial}{\partial\xi_2}\left(\frac{L_1}{L_2}\frac{\partial U}{\partial\xi_2}\right)\right]+k^2U=0. \tag{10}$$

Let us summarise our reasoning. If $L_3=1$ and the ratio L_1/L_2 is independent of ξ_3, while the function U satisfies Eqn (10), then the fields of waves of the E type are determined by the expressions

$$E_1=\frac{1}{L_1}\frac{\partial^2 U}{\partial\xi_1\partial\xi_3},\ E_2=\frac{1}{L_2}\frac{\partial^2 U}{\partial\xi_2\partial\xi_3},\ E_3=\frac{\partial^2 U}{\partial\xi_3^2}+k^2U,$$
$$H_1=-\frac{ik}{L_2}\frac{\partial U}{\partial\xi_2},\ H_2=\frac{ik}{L_1}\frac{\partial U}{\partial\xi_1},\ H_3=0. \tag{11}$$

We can show in a similar way that the fields of waves of the H type ($E_0=0$) are determined by the expressions

$$E_1=\frac{ik}{L_2}\frac{\partial V}{\partial\xi_2},\ E_2=-\frac{ik}{L_1}\frac{\partial V}{\partial\xi_1},\ E_3=0,$$
$$H_1=\frac{1}{L_1}\frac{\partial^2 V}{\partial\xi_1\partial\xi_3},\ H_2=\frac{1}{L_2}\frac{\partial^2 V}{\partial\xi_2\partial\xi_3},\ H_3=\frac{\partial^2 V}{\partial\xi_3^2}+k^2V, \tag{12}$$

and the function V satisfies the same Eqn (10). Although the function U and V entering expressions (11) and (12) are determined by the same Eqn (10), they are treated as two different Debye potentials because they describe the fields with different structures.

3. Fields of a dielectric sphere and the whispering-gallery modes (WGMs)

By using Eqn (10) and relations (11) and (12), we determine the structure of the fields of a dielectric sphere of radius a placed in vacuum. To solve this problem, it is convenient to use the spherical coordinate system r, θ, φ. Assuming that $\xi_1=\varphi$, $\xi_2=\theta$, $\xi_3=r$, we obtain $L_1=r\sin\theta$, and $L_2=r$, $L_3=1$. In this coordinate system, the conditions imposed on Lame's coefficients are satisfied (see above) at which the solutions of Maxwell's equations can be represented in the form of the E and H waves.

Equation (10) in the spherical coordinate system takes the form

$$\frac{\partial^2 U}{\partial r^2}+\frac{1}{r^2\sin\theta}\frac{\partial}{\partial\theta}\left(\sin\theta\,\frac{\partial U}{\partial\theta}\right)+\frac{1}{r^2\sin^2\theta}\frac{\partial^2 U}{\partial\varphi^2}+k^2U=0, \tag{13}$$

where $k=k_0(\varepsilon\mu)^{1/2}$ inside the sphere, $k=k_0$ outside the sphere, and $k_0=\omega/c$. Relations (11) and (12), which determine the fields, take the following form in the spherical coordinate system:

$$\left.\begin{aligned}&E_r=\left(\frac{\partial^2}{\partial r^2}+k^2\right)U,\quad H_r=0,\\&E_\theta=\frac{1}{r}\frac{\partial^2 U}{\partial r\partial\theta},\quad H_\theta=-ik\frac{1}{r}\frac{\partial U}{\partial\varphi},\\&E_\varphi=\frac{1}{r\sin\theta}\frac{\partial^2 U}{\partial r\partial\varphi},\quad H_\varphi=ik\frac{1}{r}\frac{\partial U}{\partial\theta},\end{aligned}\right\} \tag{14}$$

$$\left.\begin{aligned}&H_r=\left(\frac{\partial^2}{\partial r^2}+k^2\right)V,\ E_r=0,\\&H_\theta=\frac{1}{r}\frac{\partial^2 V}{\partial r\partial\theta},\ E_\theta=ik\frac{1}{r}\frac{\partial V}{\partial\varphi},\\&H_\varphi=\frac{1}{r\sin\theta}\frac{\partial^2 V}{\partial r\partial\varphi},\ E_\varphi=-ik\frac{1}{r}\frac{\partial V}{\partial\theta}.\end{aligned}\right\} \tag{15}$$

Let us represent the potential U in the form

$$U=R(r)\Theta(\theta)\Phi(\varphi). \tag{16}$$

By substituting (16) into (10), we obtain the following equations for the functions $R(r)$, $\Theta(\theta)$, $\Phi(\varphi)$:

$$\frac{d^2R}{dr^2}+\left(k^2-\frac{c_1}{r^2}\right)R=0, \tag{17a}$$

$$\frac{1}{\sin\theta}\frac{d}{d\theta}\left(\sin\theta\,\frac{d\Theta}{d\theta}\right)+\left(c_2-\frac{c_3}{\sin^2\theta}\right)\Theta=0, \tag{17b}$$

$$\frac{d^2\Phi}{d\varphi^2}+c_3\Phi=0, \tag{17c}$$

where c_1, c_2, c_3 are the constants appearing in the solution of equations by separating variables. The physical requirement of the uniqueness of the solutions of Eqns (17b) and (17c) leads to the relations

$$c_2=n(n+1),\ c_3=m^2, \tag{18}$$

where n and m are integers, including zero. The solutions have the form

$$\Theta(\theta)=P_n^m(\cos\theta),\ \Phi(\varphi)=\begin{cases}\sin m\varphi,\\ \cos m\varphi,\end{cases} \tag{19}$$

where $P_n^m(x)$ are the adjoint Legendre polynomials. After the substitution $R(r)=(kr)^{1/2}Z(kr)$, Eqn (17a) is transformed to the Bessel equation

$$\frac{d^2Z}{dz^2}+\frac{1}{z}\frac{dZ}{dz}+\left(1-\frac{v^2}{z^2}\right)Z=0,\ z=kr,\ v=n+\frac{1}{2}. \tag{20}$$

Physically, the solution outside the sphere should have the asymptotic form of a runaway wave, because a wave coming from infinity cannot exist. This means that the solutions outside the sphere should be expressed in terms of the Hankel functions of the first kind, which have for large arguments the asymptotic form of a runaway wave with the amplitude decreasing inversely proportional to the distance. As a result, the solution of system (14) inside the dielectric sphere ($r \leqslant a$) has the form

$$U^{\mathrm{i}}_{mn}(r,\theta,\varphi) = C_{\mathrm{i}} P^m_n(\cos\theta)(kr)^{1/2} J_\nu(kr)\mathrm{e}^{\pm \mathrm{i}m\varphi}, \tag{21}$$

and outside the dielectric sphere ($r > a$), it has the form

$$U^{\mathrm{e}}_{mn}(r,\theta,\varphi) = C_{\mathrm{e}} P^m_n(\cos\theta)(kr)^{1/2} H^{(1)}_\nu(k_0 r)\mathrm{e}^{\pm \mathrm{i}m\varphi}, \tag{22}$$

where $C_{\mathrm{i,e}}$ are arbitrary constants.

According to (14), (15), (21), and (22), it is convenient to describe the field inside ($r < a$) and outside ($r > a$) the sphere by introducing the vector spherical functions $\boldsymbol{m}_{mn}(\sigma;k)$ and $\boldsymbol{n}_{mn}(\sigma;k)$. The vectors $\boldsymbol{m}_{mn}(\sigma;k)$ and $\boldsymbol{n}_{mn}(\sigma;k)$ are presented in Tables A1.1–A1.3 in Appendix 1.

The fields of the E and H types inside the sphere are described by the expressions

$$\boldsymbol{E}_{mnq}(r,\theta,\varphi) = C_{\mathrm{i}} \boldsymbol{n}_{mn}(\sigma;k), \tag{23a}$$

$$\boldsymbol{H}_{mnq}(r,\theta,\varphi) = C_{\mathrm{i}} \boldsymbol{m}_{mn}(\sigma;k), \tag{23b}$$

$$\boldsymbol{E}_{mnq}(r,\theta,\varphi) = C_{\mathrm{i}} \boldsymbol{m}_{mn}(\sigma;k), \tag{24a}$$

$$\boldsymbol{H}_{mnq}(r,\theta,\varphi) = C_{\mathrm{i}} \boldsymbol{n}_{mn}(\sigma;k). \tag{24b}$$

The corresponding expressions for the fields outside the sphere can be obtained from expressions (23) and (24) by replacing Bessel functions $J_\nu(kr)$ by Hankel functions $H^{(1)}_\nu(k_0 r)$, and replacing the constant C_{i} by the constant C_{e}.

Note that the subscript q appears in the left-hand sides of expressions (23) and (24), which is absent in the right-hand sides. Its meaning will be explained below.

Expressions (23) and (24) should satisfy the conditions on the sphere boundary. These conditions can be satisfied after the appropriate choice of a free parameter k_{0a} and arbitrary constants $C_{\mathrm{i,e}}$. The continuity condition for the tangential components of the field at the interface between the sphere and vacuum allows one, first, to find the ratio of these constants

$$\frac{C_{\mathrm{i}}}{C_{\mathrm{e}}} = \left(\frac{1}{\varepsilon^5\mu}\right)^{1/4} \frac{H^{(1)}_\nu(k_0 a)}{J_\nu[k_0 a(\varepsilon\mu)^{1/2}]} \tag{25}$$

and, second, leads to the characteristic equations determining the admissible values of the parameter $k_0 a$. The characteristic equation for the E waves has the form

$$\frac{\left[(ka)^{1/2}J_\nu(ka)\right]'}{(ka)^{1/2}J_\nu(ka)} = \left(\frac{\varepsilon}{\mu}\right)^{1/2} \frac{\left[(k_0 a)^{1/2}H^{(1)}_\nu(k_0 a)\right]'}{(k_0 a)^{1/2}H^{(1)}_\nu(k_0 a)}, \tag{26}$$

and for the H waves, it has the form

$$\frac{\left[(ka)^{1/2}J_\nu(ka)\right]'}{(ka)^{1/2}J_\nu(ka)} = \left(\frac{\mu}{\varepsilon}\right)^{1/2} \frac{\left[(k_0 a)^{1/2}H^{(1)}_\nu(k_0 a)\right]'}{(k_0 a)^{1/2}H^{(1)}_\nu(k_0 a)}, \tag{27}$$

where the prime means a total derivative over the argument on which the function depends, i.e., over ka or $k_0 a$.

The characteristic equations determine in fact the relation between the wave number k and the sphere radius a. Because these equations have many roots, they determine an infinite set of the wave vectors (eigenfrequencies) for a given radius of the sphere. In this case, it is necessary to introduce the third index q, which indicates to what number of the root of Eqn (26) or (27) one or another value of the wave vector (eigenfrequency) corresponds. For this reason, the eigenmodes of a dielectric sphere are described by three indices m, n, q. The greater the index q (the root number), the greater number of zeroes of the function are located inside the sphere, i.e., the index q corresponds to the number of nodes of the given mode lying inside the sphere. Note that this characteristic equation is independent of the index m, so that the modes of a dielectric body of an ideal spherical shape prove to be degenerated over this index. This degeneration is removed when the shape of a dielectric body deviates from a sphere.

The boundary conditions allow us to find only the ratio of constants C_{i} and C_{e}, so that one of them remains free. It is determined by the power of sources exciting the waves. Therefore, relations (23)–(27) completely describe in principle a system of the waves inside a dielectric sphere and outside it. Which of these waves corresponds to the whispering-gallery waves (modes)?

Note first of all that the dependence of the fields on the angle φ in the form $\mathrm{e}^{\pm \mathrm{i}m\varphi}$ corresponds to the counter-propagating waves running over a circle. According to the description of Rayleigh, a whispering-gallery wave should be 'pressed down' to the sphere surface. Let us look attentively at the radial dependence of the field described by expressions (21) and (22). For a small index n, the oscillating field fills almost the entire volume of the sphere (Fig. 2). Such modes cannot be the whispering-gallery modes. However, for a large index n (for example, greater than 100), the Bessel function is very small up to $r \approx \nu/k$. For $r > \nu/k$, the Bessel function begins to oscillate with a decreasing amplitude (Fig. 3). If we choose the value of ka that is closest to the first root of the Bessel function, the field near the sphere surface will have the structure without oscillations.

We can say that the Bessel function determines the radial transverse structure of the wave. The angular transverse structure of the wave is described by the function $P^m_n(\cos\theta)$. For $m = n$, the function $P^n_n(\cos\theta)$ is proportional to $\sin^n\theta$.

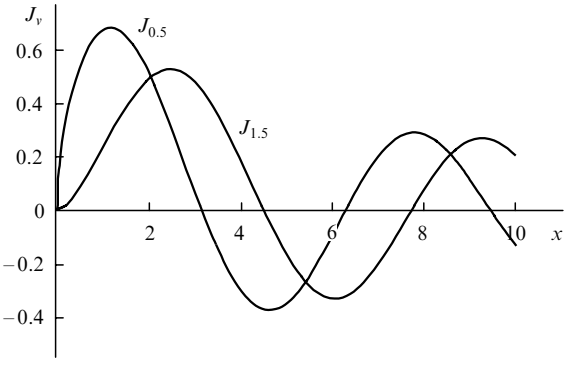

Figure 2. Bessel functions with small indices.

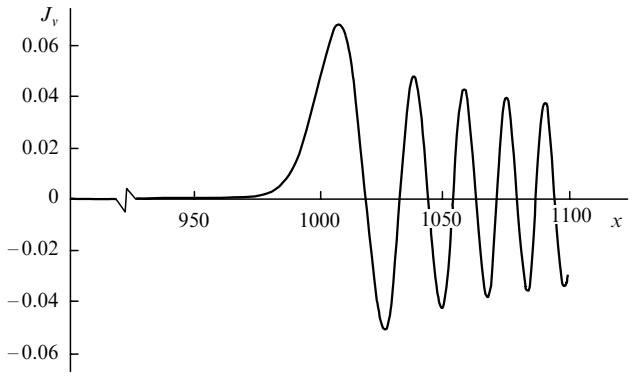

Figure 3. Bessel function with the large index $v = 1000.5$.

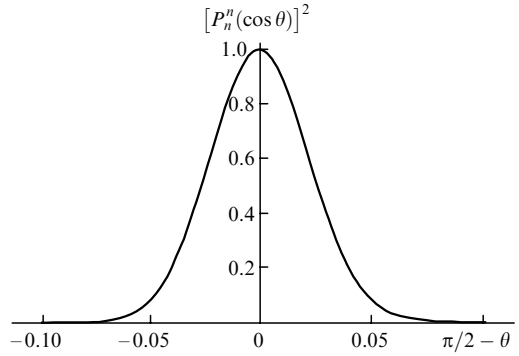

Figure 4. Function $[P_n^n(\cos\theta)]^2 \propto \sin^{2n}\theta$ for $n = 1000$.

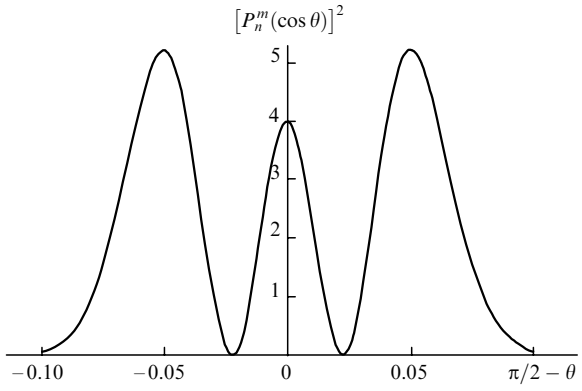

Figure 5. Function $[P_n^m(\cos\theta)]^2$ for $m = n - 2$ and $n = 1000$.

The corresponding dependence on θ is shown in Fig. 4. One can see that the field amplitude continuously decreases with increasing θ. If $m \neq n$, the mode acquires an oscillating transverse structure (Fig. 5). The oscillations increase with increasing the difference $n - m$. Therefore, it is reasonable to call a whispering-gallery mode (WGM) a wave for which the Bessel function has no roots inside a sphere and which has identical and large indices n and m. Note, however, that modes with indices $m \neq n$, but close to n, and with $q > 1$, but close to unity, have properties that are close to those of WGMs. This means that there is no a sharp difference between WGMs and other modes with nearest indices. For this reason, the modes with a small difference $n-m$ are sometimes also assigned in the literature to WGMs. We will apply the term WGM for definiteness to the modes with large indices n, $m = n$, and $q = 1$.

Note that the spherical modes are similar to the modes of Gaussian beams with a rectangular geometry [7, 8]. Indeed, a Gaussian beam is described by the Hermite–Gaussian functions $G(\xi) = H_v(\sqrt{2}\xi)\exp(-\xi^2)$, where $H_v(\sqrt{2}\xi)$ is the Hermitian polynomial and v is the integer index. These functions are the solutions of the equation

$$\frac{d^2G}{d\xi^2} + 2(2v + 1 - 2\xi^2)G = 0. \tag{28}$$

As shown above, for large indices n, the WGM field is concentrated in a narrow interval of angles θ near $\theta_0 = \pi/2$. Equation (17b) for angles θ lying within this narrow interval coincides with Eqn (28) if we set in the latter $v = n - m$ and $\xi = (n/2)^{1/2}\theta$. Thus, a spherical mode with large indices n and m and a small difference $n-m$ behaves as a Gaussian beam with the radius $w = (2/n)^{1/2}a$. Therefore, we have

$$\frac{P_n^m(\theta)}{P_n^m(0)} \approx \frac{H_{n-m}(\sqrt{n}\theta)}{H_{n-m}(0)}\exp(-n\theta^2/2). \tag{29}$$

This approximation can be rather useful in calculations because it allows one to calculate a Hermitian polynomial with small indices instead of an adjoint Legendre polynomial with large indices.

4. The evanescent WGM field

The study of the properties of WGMs involves first of all the calculation of the roots of characteristic equations. Because we deal with the modes with a large index n, it is convenient to use the appropriate approximation of Bessel functions for calculations of these roots. Note that the successful approximation is useful not only for analytic calculations but also for numerical calculations because the calculation of the Bessel functions with large indices is time-consuming. For example, to plot the function $J_{1000}(x)$ with the help of a modern PC using the Mathematica program (or similar programs like MathLab or MathCad), several hours are required.

An appropriate approximation should be chosen bearing in mind that the argument of the Bessel function for a WGM near the sphere surface is of the order of its index. In this case, the Bessel function is well approximated by Airy functions [6, 9]:

$$\sqrt{z}J_v(z) = \sqrt{2}\left(\frac{v}{2}\right)^{1/6}\mathrm{Ai}(\zeta),$$
$$\frac{d}{dz}\left[\sqrt{z}J_v(z)\right] = -\sqrt{2}\left(\frac{2}{v}\right)^{1/6}\frac{d\mathrm{Ai}(\zeta)}{d\rho}. \tag{30}$$

Because the Hankel function determines the solution outside the sphere, its argument, although remaining large, proves to be noticeably smaller than its index. In this case, the expression

$$\sqrt{z}H_z^{(1)}(z) = \sqrt{2}\left(\frac{\psi}{\sinh\eta}\right)^{1/4}\left[\mathrm{Ai}(\psi) - i\mathrm{Bi}(\psi)\right] \tag{31}$$

well approximates the Hankel function.

The functions $\mathrm{Ai}(\zeta)$ and $\mathrm{Bi}(\zeta)$ in expressions (30) and

(31) are the linearly independent solutions of the Airy equation [9]; and

$$\zeta = \left(\frac{2}{v}\right)^{1/3}(v-z);\ \eta(z) = \operatorname{arcosh}\left(\frac{v}{z}\right);$$
$$\psi = \left[\frac{3}{2}v\,(\eta - \tanh\eta)\right]^{2/3}. \tag{32}$$

The accuracy of approximations (30) and (31) is of the order of v^{-1}. If v exceeds 1000, then this accuracy is quite satisfactory for many calculations, and the time of numerical calculations decreases by hundreds times.

Expression (31) for the Hankel function allows one to calculate the field outside a sphere. When the sphere radius noticeable exceeds the wavelength, the value of ψ is large. The Airy functions with the large argument can be approximated by the expressions [10]

$$\mathrm{Ai}(\psi) \simeq \frac{1}{2}\psi^{-1/4}\exp\left(-\frac{2}{3}\psi^{3/2}\right),$$
$$\frac{\mathrm{dAi}(\psi)}{\mathrm{d}\psi} = -\frac{1}{2}\psi^{1/4}\exp\left(-\frac{2}{3}\psi^{3/2}\right), \tag{33a}$$

$$\mathrm{Bi}(\psi) \simeq \psi^{-1/4}\exp\left(\frac{2}{3}\psi^{3/2}\right),$$
$$\frac{\mathrm{dBi}(\psi)}{\mathrm{d}\psi} \simeq \psi^{1/4}\exp\left(\frac{2}{3}\psi^{3/2}\right). \tag{33b}$$

The variation of the field near the sphere surface, when $r/a - 1 \ll 1$, can be determined by expanding the argument in a Taylor series in expressions (33):

$$\frac{2}{3}\psi^{3/2} = v\left[\eta(k_0 r) - \tanh(k_0 r)\right] = v\left[L(s) - \frac{(s^2-1)^{1/2}}{s}\frac{r}{a}\right], \tag{34}$$

where

$$s = \frac{v}{k_0 a};\ L(s) = \ln\left[s + (s^2-1)^{1/2}\right]. \tag{35}$$

It follows from expressions (33)–(35) that outside the sphere, but near its surface, the imaginary part of the complex Airy function is very small, so that the field in this region is determined by the real part of this function. By substituting (34) into (33a), we find that the field exponentially falls with increasing coordinate r according to the expression

$$|E| \propto \exp\left[-2\pi(\varepsilon\mu - 1)^{1/2}\frac{r}{\lambda}\right], \tag{36}$$

where λ is the wavelength in vacuum. The expotential decay of the field amplitude at the surface vicinity makes the reason to refer this field as evanescent. This result can be also obtained by directly analysing Eqn (20). Indeed, for $r > a$, Eqn (20) near the sphere surface can be approximated as

$$\frac{\mathrm{d}^2 Z}{\mathrm{d}z^2} + \frac{1}{k_0 a}\frac{\mathrm{d}Z}{\mathrm{d}z} + \left[1 - \frac{v^2}{(k_0 a)^2}\right]Z = 0. \tag{37}$$

The solution of this equation, which decreases at infinity, has the form

$$Z(k_0 r) = \mathrm{const} \times \exp\left\{-\left[\frac{v^2}{(k_0 a)^2} - 1 + \frac{1}{4(k_0 a)^2}\right]^{1/2} - \frac{1}{2k_0 a}\right\}k_0 r. \tag{38}$$

We will show below that [see expression (45)] that $k_0 a \approx v/(\varepsilon\mu)^{1/2} \gg 1$. Taking this into account, the exponent of the exponential in (38) is approximately equal to $(2\pi/\lambda)\times(\varepsilon\mu - 1)^{1/2} r$, and we arrive at expression (36). Beginning from c $r > v/k_0 \approx (\varepsilon\mu)^{1/2} a$, the quantity $1 - v^2/(k_0 r)^2$ in (20) becomes positive, so that the solution proves to be close to a sinusoid with a slowly decreasing amplitude.

The role of the imaginary part of the Airy function increases with increasing r. The contribution of the imaginary part becomes equal to that of the real part for the radius determined by the relation $\eta(k_0 r) - \tanh\eta(k_0 r) = 0$, i.e., by the relation $\eta(k_0 r) = 0$. Taking into account the definition of the parameter $\eta(k_0 r)$ [see (32)], we find that this occurs at the distance $r \approx a(\varepsilon\mu)^{1/2}$. When the contributions from the real and imaginary parts become equal, the exponentially decreasing field transforms to a runaway wave with the amplitude that decreases inversely proportional to $\sqrt{r}$.

Because the field amplitude at distances $r > a\,(\varepsilon\mu)^{1/2}$ becomes very small, the intensity of radiation emitted from the sphere is very low. This is confirmed by the direct calculation of the WGM Q-factor. As a result, we can imagine the following picture. The WGM field occupies a volume bounded by a spherical surface of radius $a(\varepsilon\mu)^{1/2}$. Radiation is emitted outside from this volume in the form of a runaway wave with very small amplitude. However, the field occupies in fact not the entire volume of a sphere with radius $a(\varepsilon\mu)^{1/2}$ but it is 'pressed down' to the surface of the dielectric sphere, extending outside the sphere by the distance $r = \lambda/[2\pi(\varepsilon\mu - 1)^{1/2}] \ll a(\varepsilon\mu)^{1/2}$ [see (36)]. For such materials as glass and quartz, this distance is smaller than the wavelength in free space, not to mention dielectric with large ε, for example, diamond ($\varepsilon \approx 6$) or semiconductor materials ($\varepsilon > 10$). Note that in the case of semiconductors, we are dealing with radiation frequencies that are considerable lower than the frequency of interband transitions. In this case, the absorption of radiation due to the interband transitions is insignificant.

5. Roots of characteristic equations and eigenfrequencies

Consider now the roots of characteristic equations. By using relations (30)–(33), we represent Eqns (26) and (27) in terms of Airy functions to obtain

$$\frac{1}{\mathrm{Ai}(\zeta)}\frac{\mathrm{dAi}(\zeta)}{\mathrm{d}\zeta} = \left(\frac{\varepsilon}{\mu}\right)^{1/2}\left(\frac{v}{2}\right)^{1/3}\left\{\left[\frac{v}{ka}(\varepsilon\mu)^{1/2}\right]^2 - 1\right\}^{1/2}$$
$$\times\left[1 - \mathrm{i}\exp(-2T)\right],\ \zeta = \left(\frac{2}{v}\right)^{1/3}(v - ka),\ T = v(\eta - \tan\eta) \tag{39}$$

for the E waves and

$$\frac{1}{\mathrm{Ai}(t)}\frac{\mathrm{dAi}(t)}{\mathrm{d}t} = \left(\frac{\mu}{\varepsilon}\right)^{1/2}\left(\frac{v}{2}\right)^{1/3}\left\{\left[\frac{v}{ka}(\varepsilon\mu)^{1/2}\right]^2 - 1\right\}^{1/2}$$
$$\times\left[1 - \mathrm{i}\exp(-2T)\right] \tag{40}$$

for the H waves.

If the parameter v is large, so that the value of $(v/2)^{1/3}$ is also sufficiently large, we can find, following [10], the roots of Eqns (39) and (40) analytically. If v were infinitely large,

then Eqns (39) and (40) would be satisfied by the roots of the equation

$$\mathrm{Ai}(\zeta) = 0. \tag{41}$$

Let us denote the roots of this equation by ζ_q and find the correction $\Delta\zeta_q$ in the first approximation to these roots. Let us expand the right- and left-hand sides of Eqns (39) and (40) into a series with an accuracy to linear terms in $\Delta\zeta_q$ and solve then for $\Delta\zeta_q$. Then, we have

$$\Delta\zeta_q = \left(\frac{2}{v}\right)^{1/3}\left[\frac{\mu}{\varepsilon(\varepsilon\mu-1)}\right]^{1/2}\left[1+\mathrm{i}\exp(-2T_q)\right], \tag{42}$$

for Eqn (39) (the E modes)

$$\Delta\zeta_q = \left(\frac{2}{v}\right)^{1/3}\left[\frac{\varepsilon}{\mu(\varepsilon\mu-1)}\right]^{1/2}\left[1+\mathrm{i}\exp(-2T_{nq})\right], \tag{43}$$

and for Eqn (40) (the H modes) where

$$T_{nq} = v\left[\operatorname{arcosh}(\varepsilon\mu)^{1/2} - \left(\frac{\varepsilon\mu-1}{\varepsilon\mu}\right)^{1/2}\right] + \left(\frac{v}{2}\right)^{1/3} \times \rho_q\left(\frac{\varepsilon\mu-1}{\varepsilon\mu}\right)^{1/2} + \frac{1}{\varepsilon}. \tag{44}$$

Taking into account that $\zeta = (2/v)^{1/3}(v-ka)$ [see (39)], the eigenvalues of the wave numbers can be represented in the explicit form

$$k_{0nq} = \frac{v - (v/2)^{1/3}(\zeta_q + \Delta\zeta_q)}{a(\varepsilon\mu)^{1/2}}. \tag{45}$$

Because the quantity $\Delta\zeta_q$ is complex, the eigenvalues of the wave numbers are also complex. The real part of the wave number determines the eigenfrequencies of the modes. By using the numerical value of the first root of the Airy function ($\zeta_1 = -2.33811$), we present the expressions for the eigenfrequencies of WGMs to the form convenient for calculations

$$\omega_n^{\mathrm{E}} \approx \frac{c}{a(\varepsilon\mu)^{1/2}}\left[v + 1.85576v^{1/3} - \frac{1}{\varepsilon}\left(\frac{\varepsilon\mu}{\varepsilon\mu-1}\right)^{1/2} + O\left(v^{-1/3}\right)\right], \tag{46a}$$

$$\omega_n^{\mathrm{H}} \approx \frac{c}{a(\varepsilon\mu)^{1/2}}\left[v + 1.85576v^{1/3} - \frac{1}{\mu}\left(\frac{\varepsilon\mu}{\varepsilon\mu-1}\right)^{1/2} + O\left(v^{-1/3}\right)\right]. \tag{46b}$$

The symbol $O\left(v^{-1/3}\right)$ means, as usual, that the terms omitted in expressions (46) are of the order of $v^{-1/3}$.

The asymptotic expressions allowing the calculation of the positions of resonances of the modes of a dielectric sphere (DSMs) were refined in papers [11, 12]. In paper [11], the corrections $\Delta\omega_n^{\mathrm{E,H}}$ to expressions (46) are given, which allow the calculation of the WGM frequencies with higher accuracy:

$$\Delta\omega_n^{\mathrm{E}} = \frac{c}{a(\varepsilon\mu)^{1/2}}\left[\frac{3}{10\sqrt[3]{4}}1.8557^2 v^{-1/3} - \frac{\varepsilon^{3/2}}{3\sqrt[3]{2}(\varepsilon-1)^{3/2}} \times 1.8557v^{-2/3} + O(v^{-1})\right], \tag{47a}$$

$$\Delta\omega_n^{\mathrm{H}} = \frac{c}{a(\varepsilon\mu)^{1/2}}\left[\frac{3}{10\sqrt[3]{4}}1.8557^2 v^{-1/3} - \frac{3\varepsilon-2}{3\sqrt[3]{2}\sqrt{\varepsilon}(\varepsilon-1)^{3/2}} \times 1.8557v^{-2/3} + O(v^{-1})\right]. \tag{47b}$$

The WGM resonances were experimentally studied in paper [13] where an excellent agreement of the observed spectra with the prediction of the Mie theory was pointed out.

As mentioned above, the eigenfrequencies for modes with the same index n but different indices m are degenerated. This degeneration is removed when the shape of a dielectric body deviates from a sphere. For a spheroid with a small eccentricity, we can calculate a correction to the frequency using the perturbation theory. For this purpose, we will use the energy levels calculated in a slightly aspherical potential well (see p. 171 in [14]). Finally, we obtain

$$\omega_{nm} \simeq \omega_n\left[1 - \frac{\Delta a}{a}\left(2 + 3\frac{n^2-m^2}{n^2}\right)\right], \tag{48}$$

where Δa is the deviation of the minor axis of the spheroid from the initial radius of the sphere, and ω_n is determined by expressions (46). Expression (48) shows that the deviation of the shape of a dielectric body from a sphere not only removes the degeneration over the index m but also shifts the WGM frequency. This circumstance makes it possible to change the WGM frequency by weakly compressing the dielectric sphere.

The authors of papers [15, 16] demonstrated locking of the WGM frequency to the frequency of a tunable laser. The WGM frequency was tuned by the axial compression of a microsphere. Some other methods for tuning the WGM frequency were also discussed in the literature. For example, the WGM frequency tuning by drawing together two dielectric spheres was studied theoretically and experimentally in paper [17]. When the two spheres draw together, the coupling appears between them, which is caused by a near-surface field, resulting in the shift of the WGM eigenfrequencies. This shift increases with decreasing distance between spheres.

The splitting of resonance frequencies of spherical modes, which correspond to different indices m, was experimentally observed by the authors of paper [18]. They explained the splitting by a strong interaction of WGMs with a substrate on which microspheres were fixed. The authors of paper [19] measured the frequency shift and a change in the WGM Q-factor caused by a change in the sphere shape. They specified the configuration of the perturbation of the sphere shape and calculated the corrections to the WGM frequency and Q-factor caused by these perturbations.

The deviation of the shape of a dielectric body from a sphere does not remove the degeneracy in sign of m: the counterpropagating waves have the same frequencies. This type of degeneracy is removed by the coupling that appears between the frequency-degenerated waves due to their scattering. Scattering can be caused both by the sphere-surface roughness and by the inhomogeneities of the substance density. This type of scattering is commonly called the Rayleigh scattering.

6. Effect of the permittivity inhomogeneities on the WGM frequency

The authors of paper [20] observed and studied the frequency splitting of two counterpropagating WGMs. By studying the WGM resonances, they found two peaks separated by the distance that varied from 270 kHz to several megahertz, depending on a specific microsphere (Fig. 6). Unfortunately, the authors [20] have not pointed out whether these variations were related to different spherical samples of the same diameter or different splittings corresponded to spheres of different diameters. However, they claim that the splitting cannot be explained by volume (Rayleigh) scattering because the latter can only produce splitting that is ten times smaller than the observed splitting. This circumstance suggests that the frequency splitting is caused by the mutual coupling of the degenerate modes due to surface scattering. We failed to find in the literature a consistent theoretical analysis of the WGM frequency splitting caused by scattering. An attempt of such a calculation is presented below.

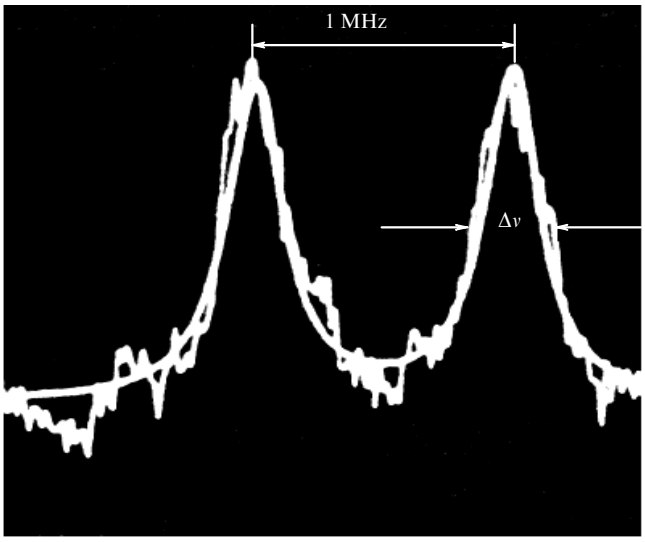

Figure 6. Frequency splitting of the (WGM caused by backscattering (experiment [20]); the peak width is $\Delta\nu = 270$ kHz.

The surface roughness, as volume inhomogeneities, can be described by introducing the fluctuations of the dielectric function of a sphere material. For this purpose, we represent the equation for the electric vector of a monochromatic field in the form

$$\nabla \times \nabla \times \boldsymbol{E}(\boldsymbol{r}) + k_0^2 \varepsilon \boldsymbol{E}(\boldsymbol{r}) = -k_0^2 \delta\varepsilon(\boldsymbol{r}) \boldsymbol{E}(\boldsymbol{r}), \tag{49}$$

by separating the fluctuating part $\delta\varepsilon(\boldsymbol{r})$ of the dielectric function. Let us define the quantity $\delta\varepsilon(\boldsymbol{r})$ so that its mean value over the sphere volume is zero. The right-hand side of this equation, under the condition $\delta\varepsilon(\boldsymbol{r}) \ll \varepsilon$, can be treated as a perturbation, and we can use the well-known method for solving such problems [14]. We assume that the degeneracy over the modulus of the index m is removed due to a small eccentricity, and consider the modes that are doubly degenerate over the sign of m. These are the waves having the same n and the same modulus of m, but counterpropagating along a major circle.

The first-order correction to the eigenfrequencies of doubly degenerated modes is described, according to [14] (p. 175, task 1), by the expression, which has in our notation the form

$$\left(\frac{\delta\omega_n^{(1)}}{\omega_n}\right)^{\mathrm{E,H}} = \frac{1}{4\varepsilon}\left\{\delta\varepsilon_{mn}^{++} + \delta\varepsilon_{mn}^{--} \pm\left[\left(\delta\varepsilon_{mn}^{++} - \delta\varepsilon_{mn}^{--}\right)^2 + 4\left|\delta\varepsilon_{mn}^{+-}\right|^2\right]^{1/2}\right\}, \tag{50}$$

where

$$\delta\varepsilon_{mn}^{ij} = \frac{1}{N_{\mathrm{E,H}}}\iiint \delta\varepsilon(\boldsymbol{r})\left\{\begin{array}{c}\boldsymbol{n}_{mn}^{i}\boldsymbol{n}_{mn}^{j*}\\ \boldsymbol{m}_{mn}^{i}\boldsymbol{m}_{mn}^{j*}\end{array}\right\}\mathrm{d}^3 r. \tag{51}$$

Each of the indices i and j in expression (51) can denote '+' or '–', and the product of vectors $\boldsymbol{n}_{mn}^{i}\boldsymbol{n}_{mn}^{j*}$ corresponds to the E modes and that of vectors $\boldsymbol{m}_{mn}^{i}\boldsymbol{m}_{mn}^{j*}$ to the H modes. The parameter $N_{\mathrm{E,H}}$ is determined by the normalisation integral. According to expressions (A1.6), (A1.7), and (A2.6), we have

$$N_{\mathrm{E,H}} = \int_0^a r^2\mathrm{d}r\int_0^\pi \sin\theta\,\mathrm{d}\theta\int_0^{2\pi}\left\{\begin{array}{c}\boldsymbol{n}_{mn}^{\pm}\boldsymbol{n}_{mn}^{\pm*}\\ \boldsymbol{m}_{mn}^{\pm}\boldsymbol{m}_{mn}^{\pm*}\end{array}\right\}\mathrm{d}\varphi = \frac{a^3}{2}\left\{\begin{array}{l}\dfrac{n+1}{2n+1}G_{\nu-1}(ka) + \dfrac{n}{2n+1}G_{\nu+1}(ka),\\ G_\nu(ka),\end{array}\right. \tag{52}$$

where

$$G_\nu(ka) = \frac{1}{ka}\left[J_\nu^2(ka) - J_{\nu-1}(ka)J_{\nu+1}(ka)\right]. \tag{53}$$

Fluctuations $\delta\varepsilon(\boldsymbol{r})$ are, as a rule, small-scale and they rapidly change compared to variations in the eigenfunctions of the dielectric sphere. Therefore, $\delta\varepsilon_{mn}^{++} = \delta\varepsilon_{mn}^{--} = 0$ because these quantities linearly depend on $\delta\varepsilon(\boldsymbol{r})$. The quantity

$$\left|\delta\varepsilon_{mn}^{+-}\right|^2 = \frac{1}{N_{\mathrm{E,H}}^2}\iiint\delta\varepsilon(\boldsymbol{r})\left\{\begin{array}{c}\boldsymbol{n}_{mn}^{+*}\boldsymbol{n}^{-}{}_{mn}\\ \boldsymbol{m}_{mn}^{+}\boldsymbol{m}_{mn}^{-*}\end{array}\right\}\mathrm{d}^3 r \times\iiint\delta\varepsilon(\boldsymbol{r}')\left\{\begin{array}{c}\boldsymbol{n}_{mn}^{+*}\boldsymbol{n}_{mn}^{-}\\ \boldsymbol{m}_{mn}^{+}\boldsymbol{m}_{mn}^{-*}\end{array}\right\}\mathrm{d}^3 r', \tag{54}$$

which is quadratic in $\delta\varepsilon(\boldsymbol{r})$, is nonzero. The method for calculating integrals with a random and rapidly changing quantity in the integrand is described, for example, in book [21]. By applying this method for the case of volume scattering, we obtain

$$\left|\delta\varepsilon_{mn}^{+-}\right|_V^2 = \frac{\langle\delta\varepsilon^2\rangle_V}{N_{\mathrm{E,H}}^2}\frac{4\pi}{3}a^3\iiint\left\{\begin{array}{c}\left|\boldsymbol{n}_{mn}^{+}\boldsymbol{n}_{mn}^{-*}\right|^2\\ \left|\boldsymbol{m}_{mn}^{+}\boldsymbol{m}_{mn}^{-*}\right|^2\end{array}\right\}\mathrm{d}^3 r. \tag{55}$$

The angle brackets mean the averaging over the sphere volume V. As a rule, volume fluctuations in a sufficiently perfect material are weaker than surface fluctuations. The thickness of a scattering surface layer is usually several nanometres, which is much smaller than the WGM layer thickness, so that

$$\left|\delta\varepsilon_{mn}^{+-}\right|_S^2 = 2\pi\frac{\langle\delta\varepsilon^2\rangle_S}{N_{\mathrm{E,H}}^2}a^4d^2\int_0^\pi\left\{\begin{array}{l}\left|\boldsymbol{n}_{mn}^{+}\boldsymbol{n}_{mn}^{-*}\right|^2\\ \left|\boldsymbol{m}_{mn}^{+}\boldsymbol{m}_{mn}^{-*}\right|^2\end{array}\right\}\sin\theta\,\mathrm{d}\theta, \quad (56)$$

where the averaging is performed over the sphere surface S, and the eigenvalues of the wave vectors in the integrand must be attributed to the surface.

Therefore, the frequency of the mode, which is degenerate in the sign of m, splits into two frequencies, which are equally shifted from the unperturbed frequency to the red and blue:

$$\left(\frac{\delta\omega_n^{(1)}}{\omega_n}\right)^{\mathrm{E,H}} = \pm\frac{d}{a}\left(\frac{\langle\delta\varepsilon^2\rangle_S}{\varepsilon^2}\right)^{1/2}D_{mn}^{\mathrm{E,H}}(ka), \quad (57)$$

where $\langle\delta\varepsilon^2\rangle_S$ is the value determined by the parameters of a rough surface. The calculation of $D_{mn}^{\mathrm{E,H}}(ka)$ is cumbersome in the general case; however, it is comparatively simple for WGMs ($m = n \gg 1$) and leads to the expressions

$$D_{nn}^{\mathrm{E}} \approx 4\left(\frac{2}{\pi}\right)^{1/2}n^{1/2}\frac{1}{ka}\frac{(n+1)J_{\nu-1}^2(ka)+nJ_{\nu+1}^2(ka)}{(n+1)G_{\nu-1}(ka)+nG_{\nu+1}(ka)}, \quad (58a)$$

$$D_{nn}^{\mathrm{H}} \approx 4\left(\frac{2}{\pi}\right)^{1/2}n^{1/2}\frac{1}{ka}\frac{J_\nu^2(ka)}{G_\nu(ka)}. \quad (58b)$$

The analysis of expressions (58) shows that the function $D_{nn}^{\mathrm{E}}(ka)$ oscillates depending on ka, but nowhere vanishes, whereas the function $D_{nn}^{\mathrm{H}}(ka)$ vanishes at the zeroes of Bessel functions. The eigenfrequencies of the H modes for large indices n prove to be close to the zeroes of Bessel functions, so that the frequency splitting for the H modes in the resonance region is very small. By tuning the resonance frequency of the H mode, the splitting can be made close to zero with high accuracy. The frequency splitting of the E mode also can be made very small by frequency tuning. The matter is that the minima of the function $D_{nn}^{\mathrm{E}}(ka)$ prove to be small for large indices n.

To excite electromagnetic oscillations in a dielectric sphere, an excitation source should be approached to the sphere (see the following sections of the review). This source introduces a perturbation into the system and can result, along with scattering, to the DSM frequency splitting. This phenomenon requires both the experimental and theoretical study.

7. The effective WGM volume

An important characteristic of a mode is its effective volume

$$V_{\kappa\eta} = \frac{\int E_{\kappa\eta}^2(\boldsymbol{r})\mathrm{d}\boldsymbol{r}}{E_{\kappa\eta}^2(\boldsymbol{r}_{\max})}, \quad (59)$$

where κ is the index of the field projection running the values of r, θ, φ; and η is the combined index (n, m, q) of the mode. The effective mode volume defined in this way is connected with a particular projection of the field and the values of this projection at the given point $r_{\max}$. The effective mode volume can be also defined differently as

$$V_\eta = \frac{\int\left[\sum\limits_\kappa E_{\kappa\eta}^2(\boldsymbol{r})+\sum\limits_\kappa H_{\kappa\eta}^2(\boldsymbol{r})\right]\mathrm{d}\boldsymbol{r}}{\sum\limits_\kappa\left(E_{\kappa\eta}^2+H_{\kappa\eta}^2\right)_{\max}}. \quad (60)$$

In this case, V_η is the characteristic of the mode as a whole. Depending on the problem being solved, expression (59) or (60) can be used. For definiteness, we will analyse in detail expression (59). The integral in (59) is reduced to a product of three integrals over the coordinates r, θ, φ. The integrals over the angles φ and θ can be calculated analytically. As a result, the effective volumes for the φ component of the field of the E mode and for the θ component of the field of the H mode have the form

$$V_{\varphi n}^{\mathrm{E}} = \pi a^3\left(\frac{\pi}{n}\right)^{1/2}\frac{1}{f_{\varphi n}^{\mathrm{E}}},\ V_{\theta n}^{\mathrm{H}} = \pi a^3\left(\frac{\pi}{n}\right)^{1/2}\frac{1}{f_{\theta n}^{\mathrm{H}}}, \quad (61)$$

where

$$\frac{1}{f_{\varphi n}^{\mathrm{E}}} = \frac{\int_0^1\left\{\frac{\mathrm{d}}{\mathrm{d}\xi'}\left[(ka\xi')^{1/2}J_\nu(ka\xi')\right]\right\}^2\mathrm{d}\xi'}{\left\{\frac{\mathrm{d}}{\mathrm{d}\xi}\left[(ka\xi')^{1/2}J_\nu(ka\xi')\right]\right\}^2\Big|_{\xi'=\xi'_{\max}}} + \frac{\int_1^{\xi'_0}\left\{\frac{\mathrm{d}}{\mathrm{d}\xi'}\left[(ka\xi')^{1/2}H_\nu^{(1)}(ka\xi')\right]\right\}^2\mathrm{d}\xi'}{\left\{\frac{\mathrm{d}}{\mathrm{d}\xi}\left[(ka\xi')^{1/2}J_\nu(ka\xi')\right]\right\}^2\Big|_{\xi'=\xi'_{\max}}} \quad (62)$$

is the radial part of integral (59) to which the φ component of the electric field of the E type from (23) is substituted; and $\xi' = r/a$. To calculate $1/f_{\theta n}^{\mathrm{H}}$, the θ component of the electric field of the H type from (24) should be substituted into integral (62). The integration in the second integral in (62) is performed up to $\xi'_0 = (\varepsilon\mu)^{1/2}$. However, this integral can be neglected because the contribution of the exponentially decaying external part of the field to the effective volume is comparatively small. As a result, by approximating the Bessel function by the Airy function, we obtain

$$\frac{1}{f_{\varphi n}^{\mathrm{E}}} \approx \left(\frac{kr_{\max}}{ka}\right)^2\frac{\int_0^1\left[\frac{\mathrm{dAi}(\zeta)}{\mathrm{d}\zeta}\right]^2\mathrm{d}\xi}{\left[\frac{\mathrm{dAi}(\zeta_{\max})}{\mathrm{d}\zeta_{\max}}\right]^2},$$
$$\frac{1}{f_{\theta n}^{\mathrm{H}}} \approx \left(\frac{kr_{\max}}{ka}\right)^2\frac{\int_0^1\mathrm{Ai}^2(\zeta)\mathrm{d}\xi}{\mathrm{Ai}^2(\zeta_{\max})}. \quad (63)$$

The effective volumes for the θ and φ components of the field are related by the expressions

$$V_{\theta n}^{\mathrm{E}} = (\mathrm{e}/2)V_{\varphi n}^{\mathrm{E}},\ V_{\varphi n}^{\mathrm{H}} = (\mathrm{e}/2)V_{\theta n}^{\mathrm{H}}, \quad (64)$$

where e is the base of natural logarithms. Here, we use only the index n as the mode index because $n = m$ and $q = 1$ for WGMs.

Along with a concept of the effective volume, we can also introduce the effective area $S_{n\varphi,n\theta}^{\mathrm{E,H}}$ and effective thickness $h_{n\varphi,n\theta}^{\mathrm{E,H}}$ of WGMs:

$$S_{n\varphi,n\theta}^{\mathrm{E,H}} = 4\pi a^2\left(\frac{\pi}{16n}\right)^{1/2},\quad h_{n\varphi,n\theta}^{\mathrm{E,H}} = \frac{a}{f_{n\varphi,n\theta}^{\mathrm{E,H}}}. \quad (65)$$

It is convenient to calculate the integrals in expression (63) numerically, by introducing the value determined by

expressions (46) as the wave number of a mode or by calculating this value by solving numerically Eqns (39) or (40) by neglecting the imaginary term in the right-hand side of the equations. We will calculate the effective volume by substituting the value of the φ component of the field on the sphere surface into the denominator in (63). The radial coordinate $r_{\max}$ corresponding to the maximum of the φ component can be calculated numerically. Table 1 presents the WGM parameters calculated for the E modes.

Table 1. The E modes.

n	ka (39)	ka (46a)	$(kr)_{\max}$	$f^{\mathrm{E}}_{\varphi n}$	$2.113n^{0.642}$
6000	6033.66	6033.67	6034.21	563	563
5000	5031.67	5031.68	5032.22	500	501
4000	4029.40	4029.40	4029.94	431	434
3000	3026.70	3026.71	3027.25	359	360
2000	2023.32	2023.33	2023.86	278	278

We assumed in the calculations that the dielectric sphere is made of quartz ($\varepsilon = 2.37$, $\mu = 1$). The second and third columns present the eigenfrequencies, which were numerically calculated from Eqn (39) or calculated from expression (46a). The radial position $(kr)_{\max}$ of the maximum of the square of the modulus of the corresponding projection is presented in the fourth column. The parameter $f^{\mathrm{E}}_{\varphi n}$ and the expression $2.113\,n^{0.642}$ approximating it are presented in the fifth and sixth columns. The approximating expression was selected empirically, and, as one can see from Table 1, well describes the dependence of $f^{\mathrm{E}}_{\varphi n}$ on the mode index n.

It follows from Table 1 that the maximum of the field determined by the Bessel function lies formally outside the sphere: $(kr)_{\max} > ka$. However, the field outside the sphere is described by the Hankel function rather than the Bessel function, and it rapidly exponentially decays with distance from the sphere, so that the field maximum for the E modes lies on the sphere surface.

The calculations described above lead to the following simple expression for the effective volume:

$$V^{\mathrm{E}}_{\varphi n} = \frac{0.63}{n^{1.142}}\left(\frac{4\pi}{3}a^3\right). \tag{66}$$

One can see that the effective WGM volume occupies only a small fraction of the total volume of the sphere and decreases approximately inversely proportional to the mode index. Table 2 presents the parameters of a WGM of the H type.

Table 2. The H modes.

n	ka (40)	ka (466)	$(kr)_{\max}$	$f^{\mathrm{H}}_{\theta n}$	$0.795n^{0.659}$	$(f^{\mathrm{H}}_{\theta n})_{\mathrm{sur}}$
6000	6032.90	6032.91	6015.13	246	246	3.44
5000	5030.91	5030.92	5014.26	218	218	3.45
4000	4028.64	4028.64	4013.26	188	188	3.48
3000	3025.95	3025.95	3012.08	156	156	3.46
2000	2022.56	2022.57	2010.59	120	119	3.44

Our calculations show that the square of the modulus of the field on the sphere surface is virtually independent of the mode index and is several tens times smaller than the square of the modulus of the field at the field maximum, which is located inside the sphere. The parameter $(f^{\mathrm{H}}_{\theta n})_{\mathrm{sur}}$ corresponding to the field on the sphere surface is small and virtually independent of the mode index, at least in the range of indices studied. The effective volume of the H mode is described by the expression

$$V^{\mathrm{H}}_{\theta n} = \frac{0.24}{n^{1.159}}\left(\frac{4\pi}{3}a^3\right). \tag{67}$$

Expressions (66) and (67) show that the effective WGM volume for large mode indices occupies only a small fraction of the total sphere volume.

8. The WGM *Q*-factor

The imaginary part of the eigenvalue of the wave number (45) determines the decay of the given mode, so that the modes of a dielectric sphere always decay. This is caused by radiation of a wave from the dielectric sphere, and therefore such a decay can be called the radiative decay. This decay is caused by the fact that, unlike a flat surface, the total internal reflection (TIR) from a curved surface does not exist. But to what extent can we assume that a WGM is formed nevertheless due to TIR? The answer to this question can be found by calculating the Q-factor of the mode caused by radiative losses. The Q-factor Q_{nq} is defined as the ratio of the real and imaginary parts of the eigenvalue of the wave number. It follows from (45) that

$$Q_{nq} = \frac{\mathrm{Re}\,k_{0nq}}{\mathrm{Im}\,k_{0nq}} = \frac{v}{2}\left[\frac{\varepsilon(\varepsilon\mu-1)}{\mu}\right]^{1/2}\exp(2T_{nq}). \tag{68}$$

Because the roots ζ_q of the Airy function are negative, the value of T_{nq} decreases with increasing the root number q. For this reason, the mode Q-factor rather rapidly decreases with increasing q. Consider a particular example for $\zeta_1 = -2.33811$ and $\zeta_2 = -4.08795$. It follows from expressions (44) and (68) that for the mode with the index $n = 2000$ and $\varepsilon = 2.37$ (quartz), Q_{n1} exceeds Q_{n2} more than by 11 orders of magnitude.

It is easy to calculate the mode Q-factor Q_{n1} for a quartz sphere ($\varepsilon = 2.37$, $\mu = 1$) for $n = 2000$. It proves to be astronomically huge, of the order of 10^{400}. The Q-factor drastically decreases with decreasing index n. For example, the radiative Q-factor for a quarts sphere for $n = 66$ is $\sim 3 \times 10^{10}$, while for $n = 60$, it is an order of magnitude lower.

It follows from expression (45) that approximate estimates at large mode indices can be performed using the expression

$$k_0 \approx \frac{v}{a(\varepsilon\mu)^{1/2}}. \tag{69}$$

To the index $n \approx 2000$ for the radius of a quartz sphere of 100 μm, the resonance frequency of the order of 3×10^{15} Hz corresponds, while the Q-factor calculated above corresponds to a fantastically huge radiative lifetime. This means that, although the internal reflection is not total, it is close to the total reflection for sufficiently large values of n. Therefore, WGMs can be treated approximately, but with very high accuracy, as TIR waves. The accuracy of this approximation increases with n.

For large values of n, the nonradiative losses determine in fact the Q-factor of the WGM. There exist other mechanisms that cause losses in WGMs. This is first of

all the scattering of an electromagnetic wave by the roughness of the sphere surface and volume scattering by the inhomogeneities of the substance density. Also, absorbing impurities can exist both inside the sphere and on its surface. In this connection, it is convenient to introduce the partial Q-factors Q_j of the mode related to each type of losses. The total mode Q-factor is described by the well-known expression

$$\frac{1}{Q} = \sum_j \frac{1}{Q_j}. \tag{70}$$

The best modern optical quartz fibres have the Rayleigh scattering coefficient of about 0.2 dB km^{-1} at the radiation wavelength of about 1.5 μm. This scattering coefficient corresponds to the Q-factor $Q_{sc} \approx 10^{11}$, which is the upper limit of the WGM Q-factor. The experimental Q-factor is much lower.

The Q-factor of the WGMs was experimentally studied in papers [20, 22, 23], where the Q-factor of quartz microspheres manufactured in vacuum was measured. The maximum WGM Q-factors of microspheres measured in vacuum were 1.4×10^9 [20], 4.9×10^9 [23] and $(8 \pm 1) \times 10^9$ [22].

A change in the WGM Q-factor upon a contact of quartz microspheres manufactured in vacuum with atmospheric air was observed in papers [22, 23]. According to the results obtained in paper [22], the Q-factor of a quartz microsphere taken out of vacuum to atmosphere decreased by a factor of 4–5 for about 4 min and then remained constant for many hours. This effect is explained by absorption of radiation by a nanolayer of molecules (first of all by water molecules) adsorbed by the microsphere surface. The authors of paper [23] confirmed this fact experimentally. It is known that the Q-factor of a resonator mode is related to the absorption coefficient $\varkappa$ of the wave intensity by the resonator medium by the expression

$$Q = \frac{2\pi}{\varkappa\lambda}(\varepsilon\mu)^{1/2}. \tag{71}$$

The partial Q-factor of a WGM of a microsphere, which is caused by absorption of radiation in a layer of absorbed molecules, can be calculated by multiplying the Q-factor (71) by the ratio δ_{ab} of the absorbing layer thickness to the effective thickness of the WGM layer. As a result, we have

$$Q_{ab}^{E,H} \approx \frac{2\pi\sqrt{\varepsilon}}{\lambda\varkappa_{ab}(\lambda)} \frac{1}{\delta_{ab}} \frac{a}{f_n^{E,H}}, \tag{72}$$

where $\varkappa_{ab}(\lambda)$ is the absorption coefficient by adsorbed water molecules.

The authors of paper [23] studied experimentally in vacuum the dependence of the WGM Q-factor on the microsphere diameter and the radiation wavelength. The sphere diameter was varied from 100 to 800 μm. Fig. 7 presents the relevant experimental data. The solid curve shows the dependence of the Q-factor on the sphere diameter calculated by the expression

$$Q_{sc} = \frac{3\varepsilon(\varepsilon+2)^2}{(4\pi)^3(\varepsilon-1)^{5/2}} \frac{\lambda^{7/2}(2a)^{1/2}}{d^2 B_{rg}^2}. \tag{73}$$

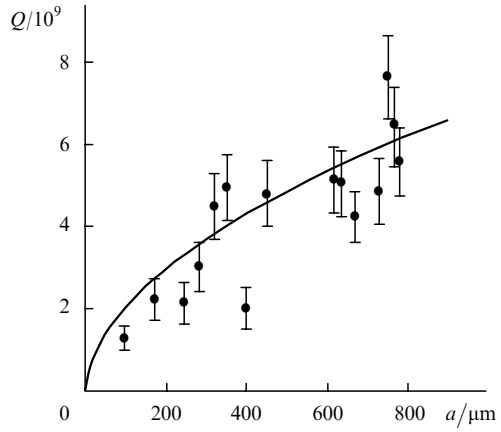

Figure 7. Experimental [23] (points) and calculated (73) dependences of the WGM Q-factor on the sphere radius a.

Here, d is the mean height of surface inhomogeneities (the scattering layer thickness) and B_{rg} is the mean size of inhomogeneities along the coordinate on the surface. Expression (73) was presented in [23] without the derivation and without references to other papers. Let us attempt to substantiate it.

The extinction coefficient $\varkappa_{sc}$ caused by scattering from the inhomogeneities of a surface can be calculated by treating the surface as an ensemble of independently scattering particles with linear sizes that are much smaller than the wavelength. Within the framework of such a model, $\varkappa_{sc} = \sigma_{sc} N$, where σ_{sc} is the scattering cross section for an electromagnetic wave by a particle, and N is the density of scattering particles. The scattering cross section calculated in paper [21] is

$$\sigma_{sc} = 24\pi^3 \left(\frac{\varepsilon-1}{\varepsilon+2}\right)^2 \frac{\Omega^2}{\lambda^4}, \tag{74}$$

where Ω is the volume of a scattering particle. For closely packed particles, the volume Ω is proportional to N^{-1}. The coefficient of proportionality should be measured experimentally; however, it is clear from the physical point of view that it is of the order of unity. Because a WGM is located within a layer whose thickness exceeds the wavelength, the effective scattering coefficient for the WGM is

$$\varkappa_{eff} = \varkappa_{sc} \frac{d}{h}, \tag{75}$$

where h is the effective thickness of the WGM layer (the mode indices at h are omitted). By substituting (75) and (65) into (71), we obtain

$$Q_{sc}^{E,H} = \frac{\sqrt{\varepsilon}}{12\pi^2} \left(\frac{\varepsilon+2}{\varepsilon-1}\right)^2 \frac{\lambda^3}{\Omega d} \frac{a}{f_n^{E,H}}. \tag{76}$$

This relation differs somewhat from expression (73). The thickness of the WGM layer in paper [23] was assumed to be $(2\lambda a)^{1/2}$, whereas in expression (76) we used a more exact value of the layer thickness. Nevertheless, for the E waves, expressions (73) and (76) give close dependences of the Q-factor on the diameter of a dielectric sphere, because $f_{n\varphi,n\theta}^{E} \propto n^{0.642}$, which is close to a square root dependence. In turn, $n \propto a$, and we see that the dependences of Q-factors

(73) and (76) on the microsphere radius are virtually identical.

For the H waves, the values of $f^{H}_{n\varphi,n\theta}$ corresponding to the surface field of the sphere are virtually independent of the mode index and, hence, of the sphere radius. Therefore, the Q-factor for WGMs of the H type should increase linearly with the sphere radius. However, the H waves are excited less efficiently because the maximum of the electric field is remote from the sphere surface.

The authors of paper [24] present, referring to paper [25], the expression

$$Q_{sc} = \frac{3}{16\delta^2}\left[\frac{\varepsilon^2}{\pi^2\lambda^4}(2a)^{10}\right]^{1/3}, \tag{77}$$

for the Q-factor of a WGM, which gives a very strong dependence on the diameter of a dielectric sphere. The experimental results [23] do not confirm this expression. Although the experimental data (Fig. 7) have a rather large statistical scatter, they undoubtedly contradict to expression (77), which gives the dependence of the Q-factor on the sphere radius in the form $(2a)^{10/3}$.

The authors of paper [23] measured also the statistical parameters of the inhomogeneous surface of silica spheres made by them and obtained $d = (1.7 \pm 0.5)$ nm and $B = (5 \pm 0.5)$ nm. The substitution of these values into expression (73) for $\lambda = 800$ nm and $a = 400$ μm gives $Q_{sc} = (7.5 \pm 5) \times 10^9$, in satisfactory agreement with the experimental value of $\sim 8 \times 10^9$. Expression (76) gives almost the same values.

Although expressions (73) and (76) satisfactorily describe the dependence of the Q-factor on the microsphere radius, they do not describe correctly the wavelength dependence of the Q-factor. Experiments performed in paper [23] showed that the Q-factor was almost independent of the wavelength in the 679–850-nm range, whereas expressions (73) and (76) predict that the Q-factor should increase more than twice when the wavelength is changed from 679 to 850 nm. Therefore, the theory of losses in WGMs should be further developed. We will present below some considerations in this respect.

In section 6, we calculated the first-order correction to the mode frequency caused by scattering. To calculate the Q-factor caused by scattering, it is necessary to take into account the second-order correction to the mode frequency. According to [14], this correction is

$$\left(\frac{\delta\omega_n^{(2)}}{\omega_n}\right)^{E,H} = \frac{k_0^2}{2\varepsilon}\sum_{n'}\frac{\delta\varepsilon_{n,n'}\delta\varepsilon_{n',n}}{k_n^2 - k_{n'}^2}. \tag{78}$$

One can see that this correction is complex because the eigenvalues k_n are complex. Therefore, $\mathrm{Re}(\delta\omega_n^{(2)}/\omega_n)^{E,H}$ determine the correction to the mode frequency in the next approximation, and the expression

$$\mathrm{Im}\left(\frac{\delta\omega_n^{(2)}}{\omega_n}\right)^{E,H} = \frac{1}{Q_{scn}} \tag{79}$$

determines the WGM Q-factor caused by scattering from the surface roughness or volume inhomogeneities of the substance density.

As mentioned above, the imaginary part k_n determines the radiative decay of a WGM. Because this decay is weak, the imaginary part k_n or $k_{n'}$ is very small for large values of n and n'. But if n' is small, then the imaginary and real parts of the eigenvalues are comparable. This means that the terms with small n' make the main contribution to the decay.

Because the eigenvalues with small indices are considerably lower than the eigenvalues with large indices, we can write approximately

$$\left(\frac{1}{Q_{scn}}\right)_{E,H} \simeq \frac{1}{\varepsilon^2}\sum_{n'}\delta\varepsilon_{nn'}\delta\varepsilon_{n'n}\frac{k'_{n'}k''_{n'}}{k'^2_{0n}}, \tag{80}$$

where $k'_{n'}$ and $k''_{n'}$ are the real and imaginary parts of the eigenvalues.

Formula (80) is a more rigorous expression for the WGM Q-factor caused by scattering than expressions (73) or (76). An analysis of (80) as a function of the wavelength and the microsphere radius requires a special, most probably, numerical study. We are not aware of any relevant publications. Our estimates show that the Q-factor (80) increases with increasing wavelength as $\sim\lambda^{1/3}$. This means that the Q-factor changes only within 10 % when the wavelength changes from 600 to 800 nm. Therefore, the wavelength dependence of the Q-factor predicted by expression (80) does not contradict to the experimental results obtained in paper [23].

The authors of paper [26] studied experimentally the lifetime of photons in ethanol drops of radius ~ 45 μm. They found a strong influence of stimulated Raman scattering on the Q-quality of modes excited in the drops.

Let us summarise the above discussion. The WGMs are distinguished among other DSMs first of all by their high Q-factor and small effective volume. The effective volume of the mode increases with decreasing index m, and for $m = 0$ it exceeds by a factor of $\sqrt{n}$ the volume of the WGM with $m = n$. As shown above, the radiative losses are independent of the index m. However, the losses caused by surface scattering increase with decreasing m because the effective area of the mode on the sphere surface increases with decreasing m. The maximum Q-factor of the WGM is restricted by the volume Rayleigh scattering and approaches $\sim 10^{11}$. However, in practice the Q-factor of the order of $(1 - 5) \times 10^9$ can be achieved, which is limited by scattering of light from the surface inhomogeneities of a dielectric sphere. In this connection, it would be interesting to perform experiments with liquid quartz drops, in which the surface scattering can be weaker than in solid microspheres.

9. Excitation of WGMs by a plane wave

The use of WGMs for solving various scientific and applied problems is closely related to the problem of their excitation. In practice, WGMs are excited by near-surface fields. These can be the fields of near-surface TIR waves, planar or fibre waveguides. The excitation of WGMs by a plane wave is not used. Experiments have shown that a plane wave cannot in fact excite WGMs. To understand why it is so, it is necessary to consider consistently the problem of excitation of WGMs by an external source.

Excitation of WGMs is a particular case of excitation of any DSMs. The problem of excitation of WGMs by a plane wave can be solved using the theory of diffraction of this wave by a dielectric sphere, which was developed by Mie [2]. The method for solving the problem used by Mie became typical for problems of this kind and it consists in the

following. An external wave is represented as a superposition of WGMs. In book [4], referring to a paper of Mie [2], the expression

$$E_x = E_0 \exp(-\mathrm{i}\omega t) \sum_1^\infty \mathrm{i}^n \left(\frac{\pi}{2}\right)^{1/2} \times \frac{2n+1}{n(n+1)} \left[\boldsymbol{m}_{1n}^{\pm}(1;k) - \mathrm{i}\boldsymbol{n}_{1n}^{\pm}(1;k)\right] \quad (81)$$

is presented for the expansion of a plane wave propagating along the z axis and polarised along the x axis. Here, we present only the electric component of the electromagnetic field because the magnetic component can be readily written by using the expression

$$\boldsymbol{H} = \mathrm{i}\frac{c}{\omega}\mathrm{rot}\boldsymbol{E} \quad (82)$$

and the relations

$$\mathrm{rot}\left[\boldsymbol{m}_{mn}^{\pm}(\sigma;k)\right] = k\boldsymbol{n}_{mn}^{\pm}(\sigma;k),\ \mathrm{rot}\left[\boldsymbol{n}_{mn}^{\pm}(\sigma;k)\right] = k\boldsymbol{m}_{mn}^{\pm}(\sigma;k). \quad (83)$$

A wave reflected from a dielectric sphere (with the index r) and a wave induced inside the sphere (with the index t) can be also presented as a superposition of the WGMs:

$$\boldsymbol{E}_{\mathrm{r}} = E_0 \exp(-\mathrm{i}\omega t) \sum_1^\infty \mathrm{i} \left(\frac{\pi}{2}\right)^{1/2} \times \frac{2n+1}{n(n+1)} \left[a\,\mathrm{r}_n \boldsymbol{m}_{1n}^{\pm}(2;k) - \mathrm{i}b_n^{\mathrm{r}}\boldsymbol{n}_{1n}^{\pm}(2;k)\right], \quad (84)$$

$$\boldsymbol{E}_{\mathrm{t}} = E_0 \exp(-\mathrm{i}\omega t) \sum_1^\infty \mathrm{i}^n \left(\frac{\pi}{2}\right)^{1/2} \times \frac{2n+1}{n(n+1)} \left[a_n^{\mathrm{t}}\boldsymbol{m}_{1n}^{\pm}(1;k) - \mathrm{i}b_n^{\mathrm{t}}\boldsymbol{n}_{1n}^{\pm}(1;k)\right]. \quad (85)$$

The coefficients $a_n^{\mathrm{r,t}}$ and $b_n^{\mathrm{r,t}}$ should be determined. To determine them, we will use the fact that the total field of the waves incident and reflected from the sphere and the field induced in the dielectric sphere should satisfy the continuity conditions for the tangential components of the electric and magnetic fields at the sphere boundary ($r = a$). These boundary conditions lead to two pairs of the inhomogeneous equations

$$a_n^{\mathrm{t}} \frac{1}{(\varepsilon\mu)^{1/2}} (ka)^{1/2} J_\nu(ka) - a_n^{\mathrm{r}} (k_0 a)^{1/2} H_\nu^{(1)}(k_0 a) = (k_0 a)^{1/2} J_\nu(k_0 a), \quad (86a)$$

$$a_n^{\mathrm{t}} \frac{1}{\mu} \left[(ka)^{1/2} J_\nu(ka)\right]' - a_n^{\mathrm{r}} \left[(k_0 a)^{1/2} H_\nu^{(1)}(k_0 a)\right]' = \left[(k_0 a)^{1/2} J_\nu(k_0 a)\right]', \quad (86b)$$

$$b_n^{\mathrm{t}} \frac{1}{\mu} (ka)^{1/2} J_\nu(ka) - b_n^{\mathrm{r}} (k_0 a)^{1/2} H_\nu^{(1)}(k_0 a) = (k_0 a)^{1/2} J_\nu(k_0 a), \quad (87a)$$

$$b_n^{\mathrm{t}} \frac{1}{(\varepsilon\mu)^{1/2}} \left[(ka)^{1/2} J_\nu(ka)\right]' - b_n^{\mathrm{r}} \left[(k_0 a)^{1/2} H_\nu^{(1)}(k_0 a)\right]' = \left[(k_0 a)^{1/2} J_\nu(k_0 a)\right]'. \quad (87b)$$

Equations (86) and (87) allow us to determine the required coefficients:

$$a_n^{\mathrm{t}} = \frac{\alpha_{n0}\beta'_{n0} - \alpha'_{n0}\beta_{n0}}{\alpha_n\beta'_{n0} - \alpha'_n\beta_{n0}},\ b_n^{\mathrm{t}} = \frac{\alpha'_{n0}\beta_{n0} - \alpha_{n0}\beta'_{n0}}{\alpha'_n\beta_{n0} - \alpha_n\beta'_{n0}}, \quad (88)$$

$$a_n^{\mathrm{r}} = -\frac{\alpha_n\alpha'_{n0} - \alpha'_n\alpha_{n0}}{\alpha_n\beta'_{n0} - \alpha'_n\beta_{n0}},\ b_n^{\mathrm{r}} = -\frac{\alpha'_n\alpha_{n0} - \alpha_n\alpha'_{n0}}{\alpha'_n\beta_{n0} - \alpha_n\beta'_{n0}}, \quad (89)$$

where we introduced for simplicity the notation

$$\alpha_n = (ka)^{1/2} J_{n+1/2}(ka),\ \alpha_{n0} = (k_0 a)^{1/2} J_{n+1/2}(k_0 a), \quad \beta_n = (ka)^{1/2} H_{n+1/2}^{(1)}(ka),\ \beta_{n0} = (k_0 a)^{1/2} H_{n+1/2}^{(1)}(k_0 a); \quad (90)$$

the prime in expressions (88) and (89) denotes the full derivative over the argument on which the function depends, i.e., over ka or $k_0 a$. Expressions (88) and (89) are called the Mie coefficients.

As follows from (84) and (85), a plane wave excites WGMs with different indices n. However, by selecting the frequency of the exciting wave closely to that of the WGM with a certain index n, we can excite predominantly the given mode. One can clearly see it from expressions (88) and (89). If the denominators in these expressions are set to zero, we obtain characteristic equations (26) and (27). This means that the real part of the denominators in expressions (88) and (89) vanishes upon substituting into them the frequency equal to the real part of the eigenvalue of the wave number (46a) or (46b). Only the imaginary part remains in the denominators in (88) and (89), which, as we have seen, is much smaller in modulus than the real part. This imaginary part corresponds to radiative losses, which are small in WGMs and do not determine the actual WGM Q-factor. For this reason, the Mie coefficients for WGMs will be strongly overstated if we retain in the denominators the imaginary part corresponding only to radiative losses. The actual Mie coefficients in the resonance region can be estimated as follows.

Let us denote the denominators in expressions (88) and (89) by $D_n^{(a,b)}(\omega)$. We expand them into a Taylor series near the resonance and take into account that $D_n^{(a,b)}(\omega'_n) = 0$ at the resonance point. Then,

$$D_n^{(a,b)}(\omega) = \left(\omega'_n - \omega + \mathrm{i}\frac{\omega'_n}{Q_n}\right) \left.\frac{\mathrm{d}D_n^{(a,b)}}{\mathrm{d}\omega}\right|_{\omega=\omega'_n}, \quad (91)$$

where ω'_n is the real part of the eigenfrequency of the mode with the index n. If Q_n is the total Q-factor of the WGM caused by any losses, we obtain for the Mie coefficients the approximate expressions, which well describe the actual excitation amplitude.

Note that expressions (84) and (85) contain the terms only with the index $m = 1$. It appears that a plane wave cannot excite the DSM with the index $m > 1$ and, hence, it cannot excite WGMs. However, this opinion is erroneous. Expressions (84) and (85) only show that the waves with the

azimuthal index $m > 1$ cannot be excited in the azimuthal plane, perpendicular to the direction of propagation of the plane wave. Let us now choose the azimuthal plane parallel to the direction of propagation of the plane wave. The angle θ in the old coordinate system is related by the expression θ', φ' with the coordinate angles in a new system.

According to the so-called addition theorem [26], the Legendre polynomials in the old coordinate system are expressed in the new system in terms of the sum of adjoint Legendre polynomials with different (including large) azimuthal indices. As a result, this sum also contains the terms with $m = n$, i.e., WGMs.

However, we will not perform cumbersome transformations of the expressions from one coordinate system to another for calculating the coefficients of excitation of WGMs by a plane wave, but consider instead the excitation of WGMs by the waves in a planar dielectric waveguide and in TIR prism. The excitation of WGMs by a plane wave will follow from the expressions obtained as a particular case.

10. Excitation of WGMs by a waveguide wave

In practice, WGMs are excited by evanescent grazing waves on the sphere surface. Such waves can be excited by using, for example, a TIR prism or a dielectric waveguide of a circular or rectangular cross section (Fig. 8). The evanescent fields in the TIR prism and waveguides exponentially decrease with distance from the prism (waveguide) surface. By changing the distance to the prism (waveguide), we can control the degree of the WGM excitation.

The problem of WGM excitation has been studied in dozens of papers, many of which have been published quite recently [27–41]. The problem of WGM excitation with the help of a waveguide or a prism could be solved by expanding the excitation wave in the eigenmodes of the combined sphere-waveguide or sphere-prism system. However, the problem of calculation of modes in a combined system is very complicated mathematically and has not been solved so far. Therefore, we should use the approximate method by neglecting the effect of the waves reflected by the sphere on the initial waves of the waveguide or prism. Consider, using this approximation, the excitation of WGMs by a wave in a plane dielectric waveguide.

Let us choose the origin of the coordinate system at the centre of the dielectric sphere (Fig. 8). According to the chosen orientation of the axes, the right-handed screw WGM has the azimuthal dependence in the form $\exp(-\mathrm{i}n\varphi)$, while the left-handed screw WGM has the azimuthal dependence in the form $\exp(\mathrm{i}n\varphi)$.

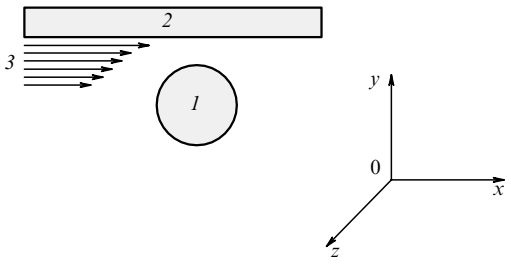

Figure 8. Scheme of excitation of a WGM by a evanescent wave in a planar waveguide; (*1*) microsphere; (*2*) planar dielectric waveguide; (*3*) near-surface waveguide wave.

The waveguide TM field near the waveguide surface facing the sphere is described by expressions [6]

$$E_x^{\mathrm{wg}} = -A\gamma \exp\left[-\gamma(l-y)\right]\exp(\mathrm{i}hx),\ H_x^{\mathrm{wg}} = 0, \tag{92a}$$

$$E_y^{\mathrm{wg}} = \mathrm{i}Ah \exp\left[-\gamma(l-y)\right]\exp(\mathrm{i}hx),\ H_y^{\mathrm{wg}} = 0, \tag{92b}$$

$$E_z^{\mathrm{wg}} = 0,\ H_z^{\mathrm{wg}} = \mathrm{i}A \exp\left[-\gamma(l-y)\right]\exp(\mathrm{i}hx), \tag{92c}$$

where A is the maximum value of the x component of the field inside the waveguide; l is the shortest distance from the sphere centre to the nearest wall of the waveguide. The wave parameters γ, g, h are related by the expressions

$$\gamma^2 + g^2 = k_0^2(\varepsilon\mu - 1),\ h^2 - \gamma^2 = k_0^2,$$
$$\gamma a_{\mathrm{p}} = \frac{1}{\varepsilon_{\mathrm{wg}}} g a_{\mathrm{p}} \begin{cases} \tan g a_{\mathrm{p}}, \\ -\cot g a_{\mathrm{p}}, \end{cases} \tag{93}$$

where $\varepsilon_{\mathrm{wg}}$ is the dielectric constant of the waveguide material and a_{p} is the thickness of the waveguide plate. The meaning of parameters γ and h follows from expressions (92). The parameter g determines the transverse structure of the field inside the waveguide. The corresponding expressions for the field inside the waveguide are not written because they will not required below. The structure of the field of a planar dielectric waveguide is described in more detail in book [6].

As shown in section 4, the amplitude of the wave of a dielectric sphere decreases by a factor of e at a distance of $r = r_{\mathrm{b}} = \lambda/[2\pi(\varepsilon\mu - 1)^{1/2}]$ from its surface. The waveguide field decays by a factor of e at a distance of $r_{\mathrm{wg}} = \gamma^{-1} = \{[2\pi(\varepsilon\mu - 1)^{1/2}/\lambda]^2 - g^2\}^{-1}$ from the waveguide boundary. One can easily see that, if the waveguide and the dielectric sphere are made of the same material, then always $r_{\mathrm{wg}} > r_{\mathrm{b}}$. Therefore, the approximation adopted above, which neglects the effect of a wave reflected from the sphere on the waveguide field, is quite real.

The first step in the expansion of the waveguide field in the spherical eigenvectors is the transformation of the field projection from the Cartesian coordinate system to the coordinate system coupled to the sphere surface. The unit vectors of the Cartesian coordinate system are expressed in terms of the unit vectors of the coordinate system coupled to the sphere as

$$\begin{aligned} \boldsymbol{e}_x &= \boldsymbol{e}_r \sin\theta\cos\varphi + \boldsymbol{e}_\theta \cos\theta\cos\varphi - \boldsymbol{e}_\varphi \sin\varphi, \\ \boldsymbol{e}_y &= \boldsymbol{e}_r \sin\theta\sin\varphi + \boldsymbol{e}_\theta \cos\theta\sin\varphi + \boldsymbol{e}_\varphi \cos\varphi, \\ \boldsymbol{e}_z &= \boldsymbol{e}_r \cos\theta - \boldsymbol{e}_\theta \sin\theta. \end{aligned} \tag{94}$$

According to these relations, the waveguide field E^{wg} (92) in the system coordinate coupled to the sphere surface has the following projections

$$E_r^{\mathrm{wg}} = B\sin\theta\exp(\mathrm{i}hx + \gamma y)(-\gamma\cos\varphi + \mathrm{i}h\sin\varphi),$$
$$H_r^{\mathrm{wg}} = \mathrm{i}B\frac{\gamma^2}{k_0}\cos\theta\exp(\mathrm{i}hx - \gamma y), \tag{95a}$$

$$E_\theta^{\mathrm{wg}} = B\cos\theta\exp(\mathrm{i}hx+\gamma y)(-\gamma\cos\varphi+\mathrm{i}h\sin\varphi),$$
$$H_\theta^{\mathrm{wg}} = -\mathrm{i}B\sin\theta\exp(\mathrm{i}hx-\gamma y), \tag{95b}$$
$$E_\varphi^{\mathrm{wg}} = B\exp(\mathrm{i}hx+\gamma y)(\gamma\sin\varphi+\mathrm{i}h\cos\varphi),$$
$$H_\varphi^{\mathrm{wg}} = 0, \tag{95c}$$

where $B = A\exp(-\gamma l)$.

Let us expand now the field (95) in the spherical vectors:

$$\boldsymbol{E}^{\mathrm{wg}} = B\exp(-\mathrm{i}\omega t)\sum_{m,n}\left[\alpha_{mn}^{\pm}\boldsymbol{m}_{mn}^{\pm}(1;k)+\beta_{mn}^{\pm}\boldsymbol{n}_{mn}^{\pm}(1;k_0)\right], \tag{96}$$
$$\boldsymbol{H}^{\mathrm{wg}} = -\mathrm{i}B\exp(-\mathrm{i}\omega t)\sum_{m,n}\left[\alpha_{mn}^{\pm}\boldsymbol{n}_{mn}^{\pm}(1;k)+\beta_{mn}^{\pm}\boldsymbol{m}_{mn}^{\pm}(1;k_0)\right],$$

where $\alpha_{mn}^{\pm}$ and $\beta_{mn}^{\pm}$ are the expansion coefficients of the waveguide field. The presence of the spherical vectors in expansion (96) only with the index $\sigma = 1$ (i.e., of Bessel functions; see Appendix 1) is caused by the fact that the amplitude of the waveguide field is finite over the entire space, so that sums in (98) cannot contain Hankel functions, which have a singularity at zero.

The coefficients $\alpha_{mn}^{\pm}$ и $\beta_{mn}^{\pm}$ are determined either by a pair of scalar products of $\boldsymbol{E}^{\mathrm{wg}}\boldsymbol{m}_{mn}^{\pm *}(1;k)$ and $\boldsymbol{E}^{\mathrm{wg}}\boldsymbol{n}_{mn}^{\pm *}(1;k)$, or $\boldsymbol{H}^{\mathrm{wg}}\boldsymbol{m}_{mn}^{\pm *}(1;k)$ and $\boldsymbol{H}^{\mathrm{wg}}\boldsymbol{n}_{mn}^{\pm *}(1;k)$, integrated over the angle θ from 0 to $-\pi$ with the weight factor $\sin\theta$ and over the angle φ from 0 to -2π. Below, we will consider only the magnetic pair because the structure of the magnetic field is simpler, according to (95).

Below, we will consider only WGMs ($m = n$), which is justified by the following circumstances. The application of DSMs most often concerns the high-Q WGMs. In a perfect spherical body, all the modes with indices $m \leqslant n$ should be excited along with WGMs. But because a real body is never a perfect sphere, the degeneracy over m is lifted [see (48)]. The relative width of the WGM resonance is $\Delta\omega_n/\omega_n = Q^{-1}$, while the relative frequency interval between the nearest modes with $m = n$ and $m = n-1$ is $\Delta\omega_{n,n-1}/\omega_n = 6(\Delta a/an)$. If the WGM Q-factor is of the order of $10^9 - 10^8$, then the difference between the neighbouring frequencies proves to be far away from the resonance even for $\Delta a/a \approx 10^{-3} - 10^{-4}$.

Let us find the scalar products required for the calculation of the coefficients of the series (96) by using relations (95) and Table A1.2. We have

$$\boldsymbol{H}^{\mathrm{wg}}\boldsymbol{n}_{nn}^{\pm *} = (-1)^{n+1}n(2n-1)!!\exp(\mathrm{i}hx+\gamma y\mp\mathrm{i}n\varphi) \times \sin^n\theta\cos\theta\,\frac{J_{\nu+1}(k_0r)}{(k_0r)^{1/2}}, \tag{97}$$

$$\boldsymbol{H}^{\mathrm{wg}}\boldsymbol{m}_{nn}^{\pm *} = \mathrm{i}(-1)^n n(2n-1)!!\exp(\mathrm{i}hx+\gamma y\mp\mathrm{i}n\varphi) \times \sin^n\theta\,\frac{J_\nu(k_0r)}{(k_0r)^{1/2}}. \tag{98}$$

To express the near-surface wave $\exp(\mathrm{i}hx+\gamma y)$ in terms of the Bessel functions, we will use the expansion [26]

$$\exp(\mathrm{i}z\sin\theta\cos\varphi) = \sum_{m=-\infty}^{\infty}\mathrm{i}^m J_m(z\sin\theta)\exp(\mathrm{i}m\varphi). \tag{99}$$

Let us transform the expression $\mathrm{i}hx+\gamma y$ so that it will be similar to the exponent in the left-hand side of equality (99):

$$\mathrm{i}hx+\gamma y = \mathrm{i}\left(h^2-\gamma^2\right)^{1/2}r\sin\theta\cos(\varphi+\mathrm{i}\psi),$$
$$\sinh\psi = \frac{\gamma}{\left(h^2-\gamma^2\right)^{1/2}}. \tag{100}$$

By substituting the expression

$$\exp\left[\mathrm{i}(h^2-\gamma^2)^{1/2}r\sin\theta\cos(\varphi+\mathrm{i}\psi)\right],$$

into the left-hand side of (99), we obtain

$$\exp(\mathrm{i}hx+\gamma y) = \sum_{m=-\infty}^{m=\infty}\mathrm{i}^m\left(\frac{h+\gamma}{h-\gamma}\right)^m J_m(k_0r\sin\theta)\exp(\mathrm{i}m\varphi). \tag{101}$$

Expression (101) is a key formula for further calculations. Scalar products (97) and (98) should be integrated over the angles φ and θ with the weight $\sin\theta$. We will call the WGM a copropagating mode if it propagates in the same direction as the excitation wave; the WGM propagating in the opposite direction will be called a counterpropagating mode. The integration over the azimuthal angle leaves in sum (101) only the terms with the index $m = n$ for the copropagating WGM and with the index $m = -n$ for the counterpropagating WGM because

$$\int_0^{2\pi}\exp(\mathrm{i}m\varphi)\exp(\mp\mathrm{i}n\varphi)\mathrm{d}\varphi = 2\pi\delta_{m,\pm n}. \tag{102}$$

For this reason, we should calculate the integrals

$$\int_0^{\pi}\sin^n\theta\cos\theta\,J_{\pm n}(k_0r\sin\theta)\mathrm{d}\theta \quad\text{and}\quad \int_0^{\pi}\sin^n\theta\,J_{\pm n}(k_0r\sin\theta)\mathrm{d}\theta.$$

By using expressions A2.7 of Appendix 2, we find

$$\int_0^{2\pi}\mathrm{d}\varphi\int_0^{\pi}\boldsymbol{H}^{\mathrm{wg}}\boldsymbol{n}_{nn}^{\pm *}\sin\theta\,\mathrm{d}\theta = 0, \tag{103}$$

$$\int_0^{2\pi}\mathrm{d}\varphi\int_0^{\pi}\boldsymbol{H}^{\mathrm{wg}}\boldsymbol{m}_{nn}^{\pm *}\sin\theta\,\mathrm{d}\theta = \mathrm{i}(-1)^n\left(\frac{\pi}{2}\right)^{1/2}n(2n-1)!!\frac{J_\nu^2(k_0r)}{k_0r}. \tag{104}$$

Now, by using (104) and expressions (A1.4) and (A1.7) of Appendix 1, we calculate the expansion coefficients

$$\beta_{nn}^{\pm} = \mathrm{i}^n(-1)^{n+1}2\pi k_0\left(\frac{\pi}{2}\right)^{1/2}\frac{2n(2n-1)!!}{2n+1}\left(\frac{h+\gamma}{h-\gamma}\right)^{\pm n/2}. \tag{105}$$

To calculate the fields excited by the waveguide field inside the sphere and outside it, we represent them in the form

$$\boldsymbol{E}_{\mathrm{t}} = E_0\exp(-\mathrm{i}\omega t)\sum_{m,n}\left[A_{mn}^{\mathrm{t}\pm}\boldsymbol{m}_{mn}^{\pm}(1;k)+B_{mn}^{\mathrm{t}\pm}\boldsymbol{n}_{mn}^{\pm}(1;k)\right], \tag{106}$$

$$\boldsymbol{E}_{\mathrm{r}} = E_0\exp(-\mathrm{i}\omega t)\sum_{m,n}\left[A_{mn}^{\mathrm{r}\pm}\boldsymbol{m}_{mn}^{\pm}(2;k)+B_{mn}^{\mathrm{r}\pm}\boldsymbol{n}_{mn}^{\pm}(2;k)\right]. \tag{107}$$

The expansion coefficients $A_{mn}^{\mathrm{r}\pm,\mathrm{t}\pm}$ and $B_{mn}^{\mathrm{r}\pm,\mathrm{t}\pm}$ are deter-

mined by the boundary conditions on the sphere surface, which lead to the equations

$$B_{nn}^{t\pm}\frac{1}{\mu}(ka)^{1/2}J_v(ka)-B_{nn}^{r\pm}(k_0a)^{1/2}H_v^{(1)}(k_0a)$$
$$=\beta_{nn}^{\pm}(k_0a)^{1/2}J_v(k_0a), \tag{108a}$$

$$B_{nn}^{t\pm}\frac{1}{(\varepsilon\mu)^{1/2}}\left[(ka)^{1/2}J_v(ka)\right]'-B_{nn}^{r\pm}\left[(k_0a)^{1/2}H_v^{(1)}(k_0a)\right]'$$
$$=\beta_{mn}^{\pm}\left[(k_0a)^{1/2}J_v(k_0a)\right]' \tag{108b}$$

for the E modes and to the equations

$$A_{nn}^{t\pm}\frac{1}{(\varepsilon\mu)^{1/2}}(ka)^{1/2}J_v(ka)-A_{nn}^{r\pm}(k_0a)^{1/2}H_v^{(1)}(k_0a)=0, \tag{109a}$$

$$A_{nn}^{t\pm}\frac{1}{\mu}\left[(ka)^{1/2}J_v(ka)\right]'-A_{nn}^{r\pm}\left[(k_0a)^{1/2}H_v^{(1)}(k_0a)\right]'=0 \tag{109b}$$

for the H modes. By solving these equations, we obtain

$$A_{nn}^{r\pm,t\pm}=A_{nn}^{r\pm,t\pm}=0, \tag{110a}$$

$$B_{nn}^{r\pm}=\beta_{nn}^{\pm}b_n^r=i^n(-1)^{n+1}$$
$$\times\frac{2n+1}{n(n+1)}\frac{2n}{(2n)!!}\left(\frac{h+\gamma}{h-\gamma}\right)^{\pm n/2}\exp(-\gamma l)b_n^r, \tag{110b}$$

$$B_{nn}^{t\pm}=\beta_{nn}^{\pm}b_n^t=i^n(-1)^{n+1}$$
$$\times\frac{2n+1}{n(n+1)}\frac{2n}{(2n)!!}\left(\frac{h+\gamma}{h-\gamma}\right)^{\pm n/2}\exp(-\gamma l)b_n^t. \tag{110c}$$

Expressions (110) demonstrate an important fact that in order to calculate the excitation coefficients of WGMs (and of DSMs in general), one should multiply the coefficient of expansion of the exciting wave over the spherical vectors by the corresponding Mie coefficient [27].

As follows from expressions (110), the TM wave of a planar dielectric waveguide does not excite WGMs of the H type. The copropagating WGM of the E type is excited by a factor of $[(h+\gamma)/(h-\gamma)]^n$ more efficiently than the counter-propagating mode. This difference can be huge for large indices n. For example, upon excitation of a wave with the parameter $k_0a\approx 3$ in a quartz waveguide plate, the value of $[(h+\gamma)/h(h-\gamma)]^n$ is $\sim(1.9)^n$.

Along with the TM waves, the TE waves can be also excited in a planar waveguide. The waveguide field of the TE type adjacent to the waveguide surface facing the sphere is described by expressions [6]

$$H_x=-A\gamma\exp[-\gamma(l-y)]\exp(ihx),\ E_x=0, \tag{111a}$$

$$H_y=iAh\exp[-\gamma(l-y)]\exp(ihx),\ E_y=0, \tag{111b}$$

$$H_z=0,\ E_z=-iA\exp[-\gamma(l-y)]\exp(ihx). \tag{111c}$$

The wave parameters γ, g, h are related by the expressions

$$\gamma^2+g^2=k_0^2(\varepsilon-1), \tag{112}$$

$$h^2-\gamma^2=k_0^2,\ \gamma a_p=ga_p\begin{cases}\tan ga_p,\\ -\cot ga_p.\end{cases}$$

The calculations, which are completely similar to the previous calculation for the TM wave, lead to the following results:

$$B_{nn}^{r\pm,t\pm}=B_{nn}^{r\pm,t\pm}=0, \tag{113a}$$

$$A_{nn}^{r\pm}=\beta_{nn}^{\pm}b_n^r=i^n(-1)^{n+1}$$
$$\times\frac{2n+1}{n(n+1)}\frac{2n}{(2n)!!}\left(\frac{h+\gamma}{h-\gamma}\right)^{\pm n/2}\exp(-\gamma l)b_n^r, \tag{113b}$$

$$A_{nn}^{t\pm}=\beta_{nn}^{\pm}b_n^t=i^n(-1)^{n+1}$$
$$\times\frac{2n+1}{n(n+1)}\frac{2n}{(2n)!!}\left(\frac{h+\gamma}{h-\gamma}\right)^{\pm n/2}\exp(-\gamma l)b_n^t. \tag{113c}$$

Therefore, the waveguide TE wave excites the WGM only of the H type. All other conclusions concerning excitation of the WGM by the waveguide TM wave are also valid for excitation by the TE wave.

The above calculations are relevant to excitation of the WGM in the azimuthal plane of the sphere, which is perpendicular to the planar waveguide plane. To calculate excitation of the WGM in the azimuthal plane of the sphere parallel to the planar waveguide plane, one should interchange the y and z components of the field in relations (92) and (111). By performing calculations, which are similar to those presented above, we find that the WGM cannot be excited in the azimuthal plane. This is reasonable according to geometrical considerations.

Consider the dependence of the quantity $[(h+\gamma)\times(h-\gamma)^{-1}]^{1/2}\equiv(h+\gamma)/k_0$ on the dielectric constant ε_{wg} of the waveguide material. It follows from relations (112) that $[(h+\gamma)/k_0]_{max}\simeq\varepsilon_{wg}^{1/2}+(\varepsilon_{wg}-1)^{1/2}$. On the other hand, the function $J_v(k_0a)$ depends on the dielectric constant of the sphere material. For large indices v and large arguments k_0a and the condition $v>k_0a$, we have

$$J_v(k_0a)\approx\frac{1}{(2\pi)^{1/2}}\left(\frac{k_0a}{v}\right)^n\approx\frac{1}{(2\pi)^{1/2}}\left(\frac{1}{\varepsilon^{1/2}}\right)^n, \tag{114}$$

and, therefore

$$\left(\frac{h+\gamma}{k_0}\right)^n J_v(k_0a)<\frac{1}{(2\pi)^{1/2}}\left[\frac{\varepsilon_{wg}^{1/2}+(\varepsilon_{wg}-1)^{1/2}}{\varepsilon^{1/2}}\right]^n. \tag{115}$$

It follows from expression (115) that, to excite the WGM efficiently, the waveguide should be made of the material whose optical density is not lower than that of the sphere material. One should also bear in mind that for WGMs with high indices, the right-hand side of inequality (115) is very sensitive to even small changes in the dielectric constant of the waveguide and sphere.

11. Excitation of WGMs by a plane wave through a TIR prism and by waves of other configurations

Excitation of the WGM by a TIR wave was studied in papers [30, 31]. The TIR wave can be formed by coupling a

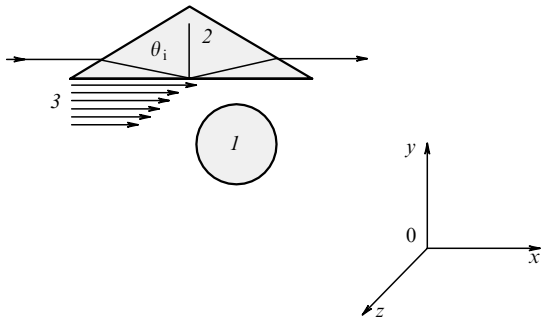

Figure 9. Scheme of excitation of a WGM by a evanescent wave in a TIR prism: (*1*) microsphere; (*2*) TIR prism; (*3*) evanescent wave in the prism; θ_i is the ange of incidence.

plane wave into a TIR prism (Fig. 9). The evanescent field of the TIR wave polarised perpendicular to the plane of incidence has the form [21]

$$E_{pz} = E_0 \frac{2\varepsilon_p^{1/2}\cos\theta_i}{\varepsilon_p^{1/2}\cos\theta_i + i(\varepsilon_p \sin^2\theta_i - 1)^{1/2}} \exp(ihx - \gamma y), \quad (116)$$

where E_0 is the amplitude of the plane wave; θ_i is the angle of incidence of the plane wave on the interface between two media; ε_p is the dielectric constant of the prism material; and

$$h = k_0\varepsilon_p^{1/2}\sin\theta_i;\ \gamma = k_0(\varepsilon_p \sin^2\theta_i - 1)^{1/2}. \quad (117)$$

This wave is similar to the TE wave in a planar waveguide. One can see from expressions (92) and (116) that the coordinate dependence of the TIR wave is similar to that of a waveguide mode of a dielectric waveguide. The projections of the TIR wave in the coordinate system fixed at the sphere surface have the form

$$E_{pr} = B\cos\theta\exp(ihx + \gamma y), \quad (118a)$$

$$E_{p\theta} = -B\sin\theta\exp(ihx + \gamma y), \quad (118b)$$

$$E_{p\varphi} = 0, \quad (118c)$$

where

$$B = E_0 \frac{2\varepsilon_p^{1/2}\cos\theta_i}{\varepsilon_p\, 1/2\cos\theta_i + i(\varepsilon_p \sin^2\theta_i - 1)^{1/2}} \exp(-i\omega t). \quad (119)$$

By projecting this field to the spherical eigenvectors, we obtain

$$\boldsymbol{E}_p \boldsymbol{n}_{nn}^{\pm *}(1;k_0) = B(-1)^n n(2n-1)!!$$
$$\times \sin^{n-1}\theta\cos\theta\exp(ihx - \gamma y \pm in\varphi)\frac{J_{v+1}(k_0 r)}{(k_0 r)^{1/2}}, \quad (120)$$

$$\boldsymbol{E}_p \boldsymbol{m}_{nn}^{\pm *}(1;k_0) = -B(-1)^n n(2n-1)!!$$
$$\times \sin^{n-1}\theta\exp(ihx - \gamma y \pm in\varphi)\frac{J_v(k_0 r)}{(k_0 r)^{1/2}}. \quad (121)$$

The integration over φ leaves only one term with $m = n$, so that

$$\int_0^{2\pi}\int_0^{\pi} \boldsymbol{E}_p \boldsymbol{n}_{nn}^{\pm}(1;k)\mathrm{d}\varphi\sin\theta\,\mathrm{d}\theta = 2\pi Bn\frac{J_{v+1}(kr)}{(kr)^{1/2}}(2n-1)!!$$
$$\times \int_0^{\pi} J_n(kr\sin\theta)\sin^n\theta\cos\theta\,\mathrm{d}\theta = 0, \quad (122)$$

$$\int_0^{2\pi}\int_0^{\pi} \boldsymbol{E}_p \boldsymbol{m}_{nn}^{+*}(1;k)\mathrm{d}\varphi\sin\theta\,\mathrm{d}\theta = 2\pi Bn\frac{J_v(kr)}{(kr)^{1/2}}(2n-1)!!$$
$$\times \int_0^{\pi} J_n(kr\sin\theta)\sin^n\theta\cos\theta\,\mathrm{d}\theta$$
$$= 4\pi Bn(2n-1)!!\left(\frac{\pi}{2}\right)^{1/2}\frac{J_v^2(kr)}{(kr)^{1/2}}. \quad (123)$$

As a result, upon excitation of the WGM by the TIR wave polarised perpendicular to the plane of incidence, we obtain

$$A_{nn}^{r\pm,t\pm} = i^n(-1)^{n+1}\left(\frac{\pi}{2}\right)^{1/2}\frac{(2n+1)}{n(n+1)}\frac{2n}{(2n)!!}$$
$$\times\left[\varepsilon_p^{1/2}\sin\theta_i + (\varepsilon_p\sin^2\theta_i - 1)^{1/2}\right]^{\pm n}\exp(-\gamma l)a_n^{r,t}, \quad (124a)$$

$$B_{nn}^{r\pm,t\pm} = 0. \quad (124b)$$

Such a wave, as we see, excites only the H waves. The magnetic field of a wave polarised in the plane of incidence has only one component, which is perpendicular to the plane of incidence (the z component in our notation). This wave is similar to the TM wave of a dielectric waveguide. All our previous reasoning and calculations applied to the magnetic field of the WGM lead to the expressions

$$A_{nn}^{r\pm,t\pm} = 0, \quad (125a)$$

$$B_{nn}^{r\pm,t\pm} = i^n(-1)^{n+1}\left(\frac{\pi}{2}\right)^{1/2}\frac{(2n+1)}{n(n+1)}\frac{2n}{(2n)!!}$$
$$\times\left[\varepsilon_p^{1/2}\sin\theta_i + (\varepsilon_p\sin^2\theta_i - 1)^{1/2}\right]^{\pm n}\exp(-\gamma l)b_n^{r,t}. \quad (125b)$$

We can obtain the coefficients of excitation of the WGM by a plane wave from expressions (123) and (124) by setting $\gamma = 0$ and $\varepsilon_p^{1/2}\sin\theta_i = 1$. For a plane wave polarised along the z axis, we have

$$A_{nn}^{r,t} = \left(\frac{\pi}{2}\right)^{1/2}\frac{2n(2n+1)}{n(n+1)(2n)!!},\ B_{nn}^{r,t} = 0, \quad (126)$$

and for a plane wave polarised along the y axis, we have

$$A_{nn}^{r,t} = 0,\ B_{nn}^{r,t} = 2\pi\left(\frac{\pi}{2}\right)^{1/2}\frac{2n(2n+1)}{n(n+1)(2n)!!}. \quad (127)$$

A comparison of expressions (123) and (124) with (126) and (127) shows that the action of the plane wave through the TIR prism enhances excitation by a factor of

$$\left[\varepsilon_{\rm p}^{1/2}\sin\theta_{\rm i}+(\varepsilon_{\rm p}\sin^2\theta_{\rm i}-1)^{1/2}\right]^{\pm n}\exp(-\gamma l). \qquad (128)$$

If the distance from the prism surface to the plate is not too large, the advantage in the excitation efficiency can be immense when the WGM index is large (1000 and more).

The features of excitation of WGMs with the help of a prism were experimentally studied in paper [7]. The light beam incident of the prism had a Gaussian shape in the cross section. As mentioned earlier, the WGM wave ($m = n$) is similar to the Gaussian beam of the fundamental mode. DSMs ($m \neq n$), which are similar to higher-order Gaussian beams, have a structure that is virtually orthogonal to that of the beam coming out of the prism and are excited very weakly. If a dielectric body has the shape of an ellipsoid of revolution, then the incidence of the Gaussian beam coming out of the prism strictly perpendicular to the rotation axis of the ellipsoid does not violate excitation of modes in the ellipsoid. However, if this beam is incident in the plane that is inclined to the ellipsoid axis at an angle less than $\pi/2$, the beam proves to be nonorthogonal to the modes with $n \neq m$, and these modes are excited along with WGMs.

When the exciting wave is incident at an angle of $\vartheta = \pm\arccos(m/n)$, the WGM is almost not excited, and only the mode with $m \neq n$ is excited. In turn, this mode excites in the prism an outgoing wave of the type of the highest mode of a Gaussian beam, which has a circular transverse structure and the transverse index $n - m$. Such a wave has the form of a circle [7] and is projected on a detector in the form of two spots, whose position is determined by angles $\vartheta = \pm\arccos(m/n)$. When the index m is even, the fundamental mode is excited along with the highest mode of a Gaussian beam.

The filament dielectric waveguides, which are similar to optical fibres used for communication, can be also employed, along with prisms and planar waveguides, for excitation of WGMs. A core of such waveguides, through which the waves propagate, is surrounded by a protective cladding, which makes difficult a contact between the waveguide and a sphere being excited. For this reason, the waveguide either is polished to form a half-block in the region of its contact with the sphere (Fig. 10) or is drawn to form a tapered waist disclosing the core at the contact (tapered fibre) [37].

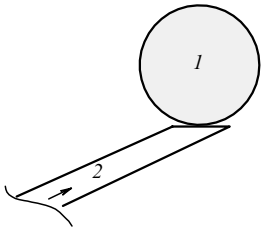

Figure 10. Scheme of excitation of a WGM by a wave in a skewed optical fibre: (*1*) microsphere; (*2*) optical fibre.

The rigorous theory of excitation of WGMs by waves in such devices is more involved mathematically than the theory of excitation by the field of a planar dielectric waveguide. However, the calculation algorithm is the same and consists in the representing of the wave in the fibre waveguide as a series in the WGM eigenfunctions. The field in a waveguide at the contact of a tapered waist with a dielectric sphere is commonly described approximately, assuming that the exciting wave is the fundamental wave of a circular dielectric waveguide [37]. The latter is described outside the waveguide by the cylindrical Hankel function [5], which can be approximated by an exponential (see section 4). As a result, the exciting field in the case of tapered fibres can be written in the form

$$E_{\rm f} = E_{\rm f0}\exp\left[-\gamma_{\rm f}(\rho - b)\right], \qquad (129)$$

where $E_{\rm f0}$ is the field near the waist surface; ρ is the radial coordinate with the centre at the fibre axis; b is the fibre radius; and

$$\gamma_{\rm f} = {\rm i}\alpha_f\frac{H_1^{(1)}({\rm i}\alpha_f b)}{H_0^{(1)}({\rm i}\alpha_f b)}. \qquad (130)$$

In turn, $\alpha_{\rm f}$ is the root of the characteristic equation [5, 37]

$$k_f\frac{J_0(k_f b)}{J_1(k_f b)} = {\rm i}\alpha_f\frac{H_1^{(1)}({\rm i}\alpha_f b)}{H_0^{(1)}({\rm i}\alpha_f b)}, \qquad (131)$$

in which

$$k_f^2 = k_0^2(\varepsilon_f - 1) - \alpha_f^2; \qquad (132)$$

and ε_f is the dielectric constant of the fibre material. In the case of a half-block, the waveguide field is more complicated [37] than field (129), and we do not consider it here.

Having the expression for the waveguide field, the problem is reduced to the representation of the fields of a microsphere and a waveguide (129) in a common coordinate system and the calculation of the coefficients of expansion of the waveguide field over spherical vectors. This problem is quite cumbersome, and we are not aware of studies where it would be consistently analysed.

Because a plane wave almost cannot excite WGMs, some studies were devoted to the analysis of excitation of WGMs by a noncentrally focused plane wave or a Gaussian beam whose axis did not pass through the sphere centre. Because these excitation methods were not used in experiments so far, we will not consider their theoretical grounds, which are reported in original papers [28, 29, 33].

12. The coupling *Q*-factor

Coupling between the fields of a sphere and a waveguide causes not only excitation of the waves in the dielectric sphere but also the energy drain from the sphere, i.e., energy losses. The relevant Q-factor is called the coupling Q-factor. To calculate the coupling Q-factor, one should solve the inverse problem of excitation of a wave in a waveguide at the expense of the energy stored in the WGM. Physically, this problem is similar to a classical problem of calculation of the damping of an oscillating dipole when the dipole emits the field whose reverse action on the dipole causes the damping of dipole oscillations [42].

A rigorous approach to the problem of excitation of waves in a waveguide or a TIR prism involves the solution of the boundary problem at the waveguide or prism surface taking into account the WGM fields. We are not aware of papers based on such an approach. Instead, the problem of

the mutual influence of the waveguide (prism) and the WGMs is solved by the following approximate method [35].

The method is based on solving Maxwell's equation

$$\left(\frac{\partial^2}{\partial t^2}+\nabla\times\nabla\times\right)\boldsymbol{E}(\boldsymbol{r},t)=-4\pi\chi(\boldsymbol{r})\frac{\partial^2\boldsymbol{E}(\boldsymbol{r},t)}{\partial t^2}, \tag{133}$$

whose solution is represented as the superposition

$$\boldsymbol{E}(\boldsymbol{r},t)=C_\eta(t)\boldsymbol{E}_\eta(\boldsymbol{r})+\sum_k C_k(t)\boldsymbol{E}_k(\boldsymbol{r}), \tag{134}$$

where $\boldsymbol{E}_\eta(\boldsymbol{r})$ and $\boldsymbol{E}_k(\boldsymbol{r})$ are the normalised fields of the modes of an isolated sphere and an excitation device. These fields satisfy the equations

$$\left[\omega_\mathrm{b}^2+\frac{c^2}{\varepsilon_\mathrm{b}(\boldsymbol{r})}\nabla\times\nabla\times\right]\boldsymbol{E}_\eta(\boldsymbol{r},t)=0,\ \varepsilon_\mathrm{b}(\boldsymbol{r})=1+4\pi\chi_\mathrm{b}(\boldsymbol{r}), \tag{135}$$

$$\left[\omega_\mathrm{p}^2+\frac{c^2}{\varepsilon_\mathrm{p}(\boldsymbol{r})}\nabla\times\nabla\times\right]\boldsymbol{E}_k(\boldsymbol{r},t)=0,\ \varepsilon_\mathrm{p}(\boldsymbol{r})=1+4\pi\chi_\mathrm{p}(\boldsymbol{r}), \tag{136}$$

where $\chi_\mathrm{b}(\boldsymbol{r})$ [or $\chi_\mathrm{p}(\boldsymbol{r})$] is constant within the sphere (or the excitation device) and is zero outside it. It is clear that the representation of the field in this form is approximate because a rigorous solution of the problem requires the calculation of the eigenfunctions of the system consisting of the sphere and the excitation device. As the excitation device, a waveguide or a prism is used. Their eigenfunctions have a continuous spectrum, so that the sum in (134) is in fact an integral.

By substituting (134) into Eqn (133) and multiplying both sides of (133) by $\boldsymbol{E}_\eta^*(\boldsymbol{r})$, we integrate the obtained expression over the effective volume of a spherical mode. As a result, we have

$$\left(\frac{\mathrm{d}^2}{\mathrm{d}t^2}+\omega_n^2\right)C_\eta(t)=-\sum_k I_k\omega^2C_k(t), \tag{137}$$

$$I_k=4\pi\left[\chi_\mathrm{b}\int\boldsymbol{E}_k(\boldsymbol{r})\boldsymbol{E}_\eta^*(\boldsymbol{r})\mathrm{d}^3r+\chi_\mathrm{p}\int\boldsymbol{E}_k(\boldsymbol{r})\boldsymbol{E}_\eta^*(\boldsymbol{r})\mathrm{d}^3r\right]. \tag{138}$$

The expression for the frequency ω_n contains the correction introduced by the excitation device, so that

$$\omega_n^2=\omega_{n0}^2-4\pi\chi_\mathrm{p}\int\left|E_\eta(\boldsymbol{r})\right|^2\mathrm{d}^3r, \tag{139}$$

where ω_{n0} is the frequency of the unperturbed spherical mode. The overlap integral (138) is small, as a rule, and can be treated as perturbation. This circumstance justifies the choice of the field in the form (134).

Let us multiply now both sides of Eqn (133) by $\boldsymbol{E}_k^*(\boldsymbol{r})$ and integrate over the effective volume of the excitation device. The obtained equation for the amplitude C_k has the form

$$\left(\frac{\mathrm{d}^2}{\mathrm{d}t^2}+\omega^2\right)C_k(t)=-I_k^*\omega_n^2C_\eta(t). \tag{140}$$

The system of equations (137) and (140) allows us to calculate the damping of the WGM caused by the coupling of the spherical modes with the excitation device. We will solve this system by the Laplace transformation method. Let us introduce the Laplace transforms $C_\eta(p)\doteq C_\eta(t)$ and $C_k(p)\doteq C_k(t)$. Then, Eqns (137) and (140) take the form

$$(p^2+\omega_n^2)C_\eta(p)=-\sum_k I_k\omega^2C_k(p)+1, \tag{141a}$$

$$(p^2+\omega^2)C_k(p)=-I_k^*\omega_n^2C_\eta(p), \tag{141b}$$

where p is the Laplace parameter. The unit in the right-hand side of the first equation corresponds to the step excitation of the WGM at the instant $t=0$. By solving the system (141), we obtain

$$C_\eta(p)=\frac{1}{p^2+\omega_n^2-\Gamma(p)},\ \Gamma(p)=\sum_k\frac{\omega^2\omega_n^2}{p^2+\omega^2}|I_k|^2. \tag{142}$$

The damping coefficient ω_n/Q_n of the WGM is determined by the real part of a pole of the function $C_\eta(p)$. Note that the calculation of $\Gamma(p)$ and poles of the function $C_\eta(p)$ is similar to that in the problem of spontaneous emission of an atom [43]. In the case of a waveguide, when only one transverse mode of the waveguide wave is resonant with the WGM, the sum in (142) is reduced to a one-dimensional integral and

$$\Gamma(p)=\mathrm{i}\pi p\omega_n^2|I_{k_n}|^2. \tag{143}$$

The calculation of the pole of the function $C_\eta(p)$ in the approximation $\Gamma(p)\ll\omega_n^2$ leads to the expression

$$\frac{\omega_n}{Q_n}=\frac{\pi}{2}\omega_n^2|I_{k_n}|^2 \tag{144}$$

for the coupling Q-factor. Now, the problem is reduced to the calculation of the overlap integrals entering (138). The corresponding calculations were performed in papers [35, 37]. We present here the expression for the coupling Q-factor for the case of excitation of the WGM by a wave of a planar waveguide [35]:

$$Q_n=\frac{4\pi^2\varepsilon_\mathrm{b}^2\varepsilon^{1/2}}{(\varepsilon_\mathrm{p}-1)^2}(\varepsilon_\mathrm{b}-1)^{3/2}\frac{a_\mathrm{p}^3}{\lambda^4}\times\exp\left[\frac{2\pi}{\lambda}l(\varepsilon_\mathrm{b}-1)^{1/2}+\frac{(n-ha)^2}{\gamma a}\right], \tag{145}$$

where a_p is the thickness of the waveguide plate; l is the distance between a sphere of radius a and the waveguide plate; and h and γ are the parameters of the waveguide wave introduced in section 10.

13. Dynamic equations for the WGM amplitudes

The applications of WGMs necessitate the analysis of nonstationary dynamic processes of excitation of WGMs by external sources.

This problem can be solved by using expressions (110), (113), (124), and (125) assuming that they were obtained for the Fourier trasforms of the relevant quantities or Laplace transforms if ω and k_0 are complex quantities. In other words, if we expand the excited field of a dielectric sphere in a series over the WGM eigenfunctions, but with coefficients depending on time

$$\boldsymbol{E}(\boldsymbol{r},t)=\sum_\eta\left[C_\eta^{\boldsymbol{m}}(t)\boldsymbol{m}_\eta+C_\eta^{\boldsymbol{n}}(t)\boldsymbol{n}_\eta\right], \tag{146}$$

then

$$C_\eta^{\boldsymbol{m},\boldsymbol{n}}(t) = q_n \int_{-\omega}^{\infty} K_\eta^{\boldsymbol{m},\boldsymbol{n}}(\omega) E_{\text{ext}}(\omega) \exp(\mathrm{i}\omega t)\mathrm{d}\omega, \tag{147}$$

where $E_{\text{ext}}(\omega) = \int E_{\text{ext}}(t)\exp(-\mathrm{i}\omega t)\mathrm{d}t$; $E_{\text{ext}}(t)$ is the field of the excitation device; and the indices at the spherical vectors $\boldsymbol{m}_{mn}^{\pm}$ and $\boldsymbol{n}_{mn}^{\pm}$ are omitted for simplicity. In the case of the TM wave of a planar waveguide [see (110)], we have

$$q_n \equiv \left(\frac{\pi}{2}\right)^{1/2} \mathrm{i}^n \frac{2n+1}{n(n+1)} \frac{2n}{(2n)!!},$$
$$K_\eta^{\boldsymbol{m},\boldsymbol{n}}(\omega) \equiv \left(\frac{h+\gamma}{k_0}\right)^{\pm n} \exp(-\gamma l) \begin{cases} a_n^{\mathrm{t}}(\omega), \\ b_n^{\mathrm{t}}(\omega). \end{cases} \tag{148}$$

To solve some problems, it is convenient to replace the integral representation of the solution (147) by the corresponding differential equation. It follows from (147) that

$$\left(\frac{\mathrm{d}^2}{\mathrm{d}t^2} + \omega_n^2\right) C_\eta^{\boldsymbol{m},\boldsymbol{n}} = q_n \int_{-\omega}^{\infty} (\omega_n^2 - \omega^2) \times K_\eta^{\boldsymbol{m},\boldsymbol{n}}(\omega) E_{\text{ext}}(\omega) \exp(\mathrm{i}\omega t)\mathrm{d}\omega. \tag{149}$$

Although the coefficients a_n^{t} and b_n^{t} have different resonance properties, for $\omega = \omega_n'$, the difference $\omega_n^2 - \omega^2$ makes the product $(\omega_n^2 - \omega^2)K_\eta^{\boldsymbol{m},\boldsymbol{n}}(\omega) \equiv \bar{K}_\eta^{\boldsymbol{m},\boldsymbol{n}}(\omega)$ a continuous function of frequency. If a signal from an external source is sufficiently monochromatic, then

$$\int_{-\omega}^{\infty} \bar{K}_\eta^{\boldsymbol{m},\boldsymbol{n}}(\omega) E_{\text{ext}}(\omega) \exp(\mathrm{i}\omega t)\mathrm{d}\omega \approx \bar{K}_\eta^{\boldsymbol{m},\boldsymbol{n}}(\omega_{\max}) E_{\text{ext}}(t), \tag{150}$$

where $\omega_{\max}$ is the frequency corresponding to the maximum of $E_{\text{ext}}(\omega)$. In addition, $\omega_n^2 = \omega_n'^2 - \gamma_n^2 - 2\mathrm{i}\omega_n'\gamma_n = \Omega_n^2 - 2\mathrm{i}\omega_n'\gamma_n$, and we have, with an accuracy to the terms of the higher order of smallness in γ_n/ω_n,

$$-2\mathrm{i}\omega_n'\gamma_n C_\eta^{\boldsymbol{m},\boldsymbol{n}} \approx 2\gamma_n \frac{\mathrm{d}C_\eta^{\boldsymbol{m},\boldsymbol{n}}}{\mathrm{d}t}. \tag{151}$$

As a result, we can write the differential equation (149) for $C_\eta^{\boldsymbol{m},\boldsymbol{n}}$ in a standard form

$$\left(\frac{\mathrm{d}^2}{\mathrm{d}t^2} + 2\gamma_n \frac{\mathrm{d}}{\mathrm{d}t} + \Omega_n^2\right) C_\eta^{\boldsymbol{m},\boldsymbol{n}} = q_n \bar{K}_\eta^{\boldsymbol{m},\boldsymbol{n}}(\omega_{\max}) E_{\text{ext}}(t). \tag{152}$$

To take into account the frequency shift and the intermode coupling due to scattering, a model of two coupled modes is used. For example, in paper [44] devoted to the stabilisation of a semiconductor laser with the help of WGMs, a model was used described by the equations

$$\frac{\mathrm{d}E_{\mathrm{L}}}{\mathrm{d}t} + \frac{1}{2\tau}(1+\mathrm{i}\Delta)E_{\mathrm{L}} - \frac{1}{2\tau}(1+\mathrm{i}\alpha)g(n_{\mathrm{e}})E_{\mathrm{L}} = \frac{1}{2}K_1 C_-(t-\tau_1)\exp(\mathrm{i}\omega\tau_1), \tag{153a}$$

$$\frac{\mathrm{d}n_{\mathrm{e}}}{\mathrm{d}t} + \frac{1}{\tau_{\mathrm{s}}}n_{\mathrm{e}} = J - g_{\mathrm{a}}(n_{\mathrm{e}})\frac{|E_{\mathrm{L}}|^2}{8\pi\hbar\omega}, \tag{153b}$$

$$\frac{\mathrm{d}C_-}{\mathrm{d}t} + \frac{1}{2\tau_0}(1+\mathrm{i}\delta)C_- = \frac{\mathrm{i}}{2}k_{\mathrm{c}}C_+, \tag{153c}$$

$$\frac{\mathrm{d}C_+}{\mathrm{d}t} + \frac{1}{2\tau_0}(1+\mathrm{i}\delta)C_+ = \frac{\mathrm{i}}{2}k_{\mathrm{c}}C_- + \frac{1}{2}K_2 E_{\mathrm{L}}(t-\tau_1)\exp(\mathrm{i}\omega\tau_1), \tag{153d}$$

where E_{L} is the complex amplitude inside the laser; n_{e} is the electron concentration in the conduction band; J is the pump-current density; ω is the frequency generated by the laser–external microresonator system; C_+ and C_- are the complex amplitudes of the fields of direct and opposite WGM waves; τ is the decay time of the field in the resonator; τ_1 is the passage time of a signal from the laser to the microsphere; τ_0 is the decay time of the WGM determined by total losses; τ_{s} is the relaxation time of the inverse population in the laser; $g_{\mathrm{a}}(n_{\mathrm{e}})$ is the gain of the laser active medium; $(1+\mathrm{i}\alpha)g_{\mathrm{a}}(n_{\mathrm{e}})$ is the complex gain of the laser active medium; ω_{c} is the eigenfrequency of the laser resonator for $g = 0$; $\Delta \equiv (\omega_{\mathrm{c}} - \omega)\tau$ and $\delta \equiv (\omega_0 - \omega)\tau_0$ are the normalised detunings; ω_0 is the WGM frequency; K_1 and K_2 are the coupling coefficients of the laser field with the WGMs, which are similar to coefficients determined, for example, by expressions (110), (113), (124), and (125); and k_{c} is the coefficient of coupling of the direct and opposite WGM waves due to scattering. It is well known that the model (153) predicts the splitting of equal resonance mode frequencies into two frequencies: $\omega_n^{\pm} = \omega_n \pm k_{\mathrm{c}}$. For this reason, $k_{\mathrm{c}}/\omega_n = \delta\omega_n^{(1)}/\omega_n$ and is determined by expression (57).

14. Applications of WGMs

Of interest are historical paradoxes: when the first lasers were developed, the researchers apprehended that WGMs in dielectric rods would prevent the outcoupling of laser radiation in the form of a highly directed beam. This concern was not in vain. To eliminate WGMs in laser rods, the side surface of the latter was purposely made rough (mat). This technology is still being used. However, at present WGMs attract attention as high-Q resonances. In the optical wavelength range, WGMs with large indices n and, therefore, with a weak radiative decay can be excited even in small spheres. It was shown that losses of other types are also rather small in spheres of radius of about 100 μm and above, so that the Q-factor can be 10^9 and higher. The possibility of obtaining high-Q WGMs even in small dielectric spheres stimulated great interest to such spheres as resonators of the optical range for the development of lasers of a new type.

WGM lasers. It seems that the first cw WGM laser was described in paper [45]. A sphere made of a Nd:YAG crystal was used both as the laser resonator and its active medium. A dye laser was used for pumping. The author of paper [45] obtained single-frequency lasing at 1064 nm.

The fabrication of a similar laser was reported in paper [46]. The spherical laser made of an Er:Yb phosphate glass was pumped through an optical fibre. The laser radiation at 1500 nm was outcoupled through the same fibre. The authors of paper [46] pointed out that the optical fibre provided not only efficient pumping and outcoupling of laser radiation but also facilitated the development of single-mode lasing.

These studies were further developed in experiments with a spherical laser made of quartz doped with neodymium atoms [47]. The authors of paper [47] fabricated a low-

threshold laser requiring near the lasing threshold only 200 nW of the pump power. The active medium of such a laser at liquid helium temperature can consist of only several neodymium atoms.

The logical development of these investigations is papers [48 – 50] in which the possibility of creating a WGM laser using one quantum dot as the active medium was substantiated. Such lasers represent objects with extremely manifested quantum properties, which make them interesting for studying the fundamental properties of radiation. It is for this reason that one-atom lasers attract the attention of theorists [51 – 53].

At present, Bose condensates of atoms captured by traps attract great attention of researchers (see, for example, [54] and references therein). The emission properties of Bose condensates can be studied by using various WGM schemes. An example of such a scheme is presented in Fig. 11.

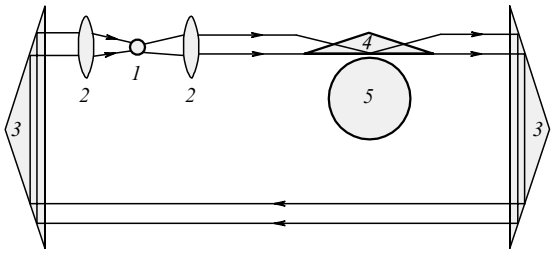

Figure 11. Possible scheme of a WGM laser with an active medium of trapped atoms: (*1*) cell with trapped cold atoms; (*2*) focusing lenses; (*3*) TIR prisms; (*4*) prism for excitation of WGMs; (*5*) silica microsphere. The light wave can propagate both clockwise and counterclockwise; a nonreciprocal element can be inserted, if necessary.

The authors of paper [55] described semiconductor lasers with resonators made of microdisks. The use of a microdisk is not unexpected because the WGM with a large index occupies a small angular aperture, and parts of a sphere outside this aperture can be removed to form a disk. The main attention in analysis of microdisk lasers was paid to their applications in optoelectronic systems for data processing [56 – 58].

The dynamics of WGM lasers was theoretically studied in papers [59 – 61].

Of interest are the experimental [62, 63] and theoretical [64, 65] papers in which lasers with liquid drops as the active medium were studied. The references in this field are cited in [61]. Note especially paper [63] where a three-colour WGM laser based on drops of dye solutions was described.

Nonlinear optical phenomena. The prospects of using WGMs for the observation of nonlinear optical phenomena were discussed in papers [24, 65]. The experimental studies of stimulated Raman scattering in drops are described in papers [66, 67]. The authors of paper [67] observed the suppression of direct lasing caused by stimulated Raman scattering. In paper [68], two-photon absorption in microsphere was studied. It seems that interest in nonlinear optics in microspheres will increase with time.

A bistable element. The possibility of using WGMs in optically bistable elements was considered in paper [24]. A small effective volume of WGMs allows the reduction of power required for a bistable element. The properties of a bistable optical element based on WGMs in a semiconductor microsphere were analysed in paper [69].

Stabilisation of diode lasers. It is known that semiconductor diode lasers have many attractive properties, which provided their wide applications. Nevertheless, they have their own disadvantages. The emission spectrum of even single-mode semiconductor laser is comparatively broad and its lasing frequency is not sufficiently stable for performing high-precision frequency measurements. Although the stabilisation of the lasing frequency and narrowing of the emission spectrum of diode lasers with the help of a standard linear resonator was successful [70, 71], a miniature semiconductor laser was transformed in this case to a rather bulky device. The use of WGMs for this purpose makes it possible to fabricate a miniature diode laser emitting highly monochromatic radiation with high frequency stability [72].

A sensitive miniature spectroscope. A high Q-factor of WGMs makes it possible to develop a highly sensitive spectroscope based on a dielectric microsphere coupled with a laser for remote sensing of traces of various gases in atmosphere [73].

Quantum electrodynamics. A high Q-factor and a small effective volume of WGMs provide their application in nondestructive quantum measurements and ensure the observations of subtle quantum effects of the interaction of single atoms with the field at the energy density equivalent to a few photons [74 – 78].

Total external reflection waves. When radiation is incident on a curved metal surface at a sufficiently large angle (grazing incidence), a wave can appear, which is almost completely similar to a WGM, but which should be called a total external reflection wave (Fig. 12). Such waves prove to be rather useful for deflecting soft X-rays by large angles. The matter is that it is almost impossible to deflect X-rays by reflecting them from a flat surface of a homogeneous material because of a low dielectric constant of almost all materials in the X-ray region. This problem is comprehensively considered in papers [79, 80].

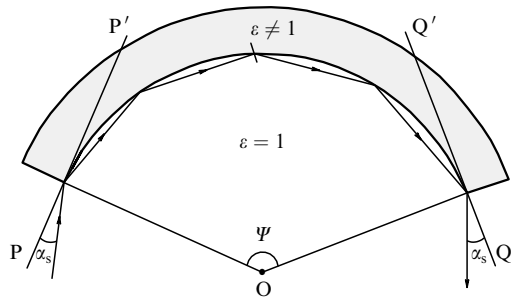

Figure 12. WGM near the surface of a concave mirror. The arrows show the directions of the entrance and exit of the wave; O is the centre of curvature of the mirror; α_s is the glancing angle; PP′ and OQ′ are the tangentials to the mirror surface.

Other types of spherical modes. As follows from section 2, the theory of spherical modes describes both WGMs and other types of spherical modes. However, in this review the main attention was devoted to modes with large indices and, hence, with low radiative losses. Nevertheless, low-index modes play an important role in the theory of scattering of light by small particles [81]. The emission properties of atoms or molecules located near small particles can be drastically changed. This and other interesting problems,

which are closely related to the theory of spherical modes, are considered in papers [82, 83].

The examples presented above do not exhaust all the possibilities of applications of WGMs. We can expect new and ingenious proposals for applications of WGMs.

Appendix 1. Vector spherical functions

It is known that Maxwell's equations in an arbitrary coordinate system can be reduced to the solution of the equation for the vector function $\boldsymbol{F}$

$$\operatorname{rotrot}\boldsymbol{F} - k^2\boldsymbol{F} = 0, \tag{A1.1}$$

where $\boldsymbol{F}$ is the electric or magnetic field. In the case of spherical fields, any vector function, which is the solution of Eqn (A1.1), can be represented as a series in the fundamental vector functions of three types [4], which are presented in Tables A1.1 – A1.3.

Table A1.1.

Ort	$\boldsymbol{m}^{\pm}_{mn}(\sigma;k)$
$\boldsymbol{e}_r$	0
$\boldsymbol{e}_\theta$	$\dfrac{m}{\sin\theta}P_n^m(\cos\theta)\dfrac{(kr)^{1/2}Z_\nu(kr)}{kr}\exp(\pm\mathrm{i}m\varphi)$
$\boldsymbol{e}_\varphi$	$\pm\mathrm{i}\dfrac{\mathrm{d}}{\mathrm{d}\theta}P_n^m(\cos\theta)\dfrac{(kr)^{1/2}Z_\nu(kr)}{kr}\exp(\pm\mathrm{i}m\varphi)$

Table A1.2.

Ort	$\boldsymbol{n}^{\pm}_{mn}(\sigma;k)$
$\boldsymbol{e}_r$	$n(n+1)P_n^m(\cos\theta)\dfrac{(kr)^{1/2}Z_\nu(kr)}{(kr)^2}\exp(\pm\mathrm{i}m\varphi)$
$\boldsymbol{e}_\theta$	$\dfrac{\mathrm{d}}{\mathrm{d}\theta}\left[P_n^m(\cos\theta)\right]\dfrac{1}{kr}\dfrac{\mathrm{d}}{\mathrm{d}(kr)}\left[(kr)^{1/2}Z_\nu(kr)\right]\exp(\pm\mathrm{i}m\varphi)$
$\boldsymbol{e}_\varphi$	$\pm\mathrm{i}\dfrac{m}{\sin\theta}P_n^m(\cos\theta)\dfrac{1}{kr}\dfrac{\mathrm{d}}{\mathrm{d}(kr)}\left[(kr)^{1/2}Z_\nu(kr)\right]\exp(\pm\mathrm{i}m\varphi)$

Table A1.3.

Ort	$\boldsymbol{l}^{\pm}_{mn}(\sigma;k)$
$\boldsymbol{e}_r$	$P_n^m(\cos\theta)\dfrac{\mathrm{d}}{\mathrm{d}(kr)}\left[\dfrac{Z_\nu(kr)}{(kr)^{1/2}}\right]\exp(\pm\mathrm{i}m\varphi)$
$\boldsymbol{e}_\theta$	$\dfrac{\mathrm{d}}{\mathrm{d}\theta}\left[P_n^m(\cos\theta)\right]\dfrac{Z_\nu(kr)}{(kr)^{3/2}}\exp(\pm\mathrm{i}m\varphi)$
$\boldsymbol{e}_\varphi$	$\pm\mathrm{i}\dfrac{m}{\sin\theta}P_n^m(\cos\theta)\dfrac{Z_\nu(kr)}{(kr)^{3/2}}\exp(\pm\mathrm{i}m\varphi)$

In these tables, $\boldsymbol{e}_r, \boldsymbol{e}_\theta, \boldsymbol{e}_\varphi$ are the unit vectors directed along the axes of the coordinate system fixed at the sphere surface (see Fig. A1.1); and $Z_\nu(kr)$ is the solution of the Bessel equation. This can be either the Bessel function $J_\nu(kr)$ or the Hankel function $H_\nu^{(1,2)}(kr)$ of the first or second kind. The index σ is introduced to indicate what of these functions is meant as $Z_\nu(kr)$. The values of $\sigma = 1, 2$, and 3 correspond to the Bessel function $J_\nu(kr)$, the Hankel function $H_\nu^{(1)}(kr)$ of the first kind, and the Hankel function $H_\nu^{(2)}(kr)$ of the second kind, respectively. The indices m, n are clear without additional comments. The symbols '$\pm$' correspond to signs '$\pm$' in the azimuthal factor $\mathrm{e}^{\pm\mathrm{i}m\varphi}$ in the potential (21). This potential serves as a base function for constructing spherical vectors $\boldsymbol{m}^{\pm}_{mn}(\sigma;k), \boldsymbol{n}^{\pm}_{mn}(\sigma;k)$ and $\boldsymbol{l}^{\pm}_{mn}(\sigma;k)$ [4].

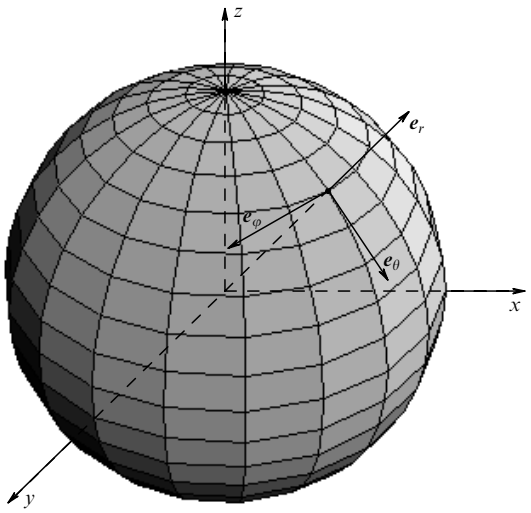

Figure 13. Coordinate system with the unit vectors $\boldsymbol{e}_r$, $\boldsymbol{e}_\theta$, $\boldsymbol{e}_\varphi$, coupled with the sphere surface.

Let us comment the notation used. In a book of Stratton [4], spherical vectors are written using the functions

$$z_n(z) = \left(\frac{\pi}{2z}\right)^{1/2} Z_\nu(z),$$

whereas Vainshtein [10] uses another notation, namely,

$$z_n(z) = \left(\frac{\pi z}{2}\right)^{1/2} Z_\nu(z).$$

Each of the authors has his own arguments in favour of the notation used by him. However, a comparison of formulas taken from the books cited above and from other sources leads to confusion. For this reason, no new notation for radial functions has been introduced in this review, and vector spherical functions are written using a standard notation of functions representing the solutions of the Bessel equation.

The spherical vectors $\boldsymbol{m}^{\pm}_{mn}$, $\boldsymbol{n}^{\pm}_{mn}$, and $\boldsymbol{l}^{\pm}_{mn}$ have the following properties:: $\operatorname{rot}\boldsymbol{l}^{\pm}_{mn} = 0$, i.e., l describes potential fields; the vectors $\boldsymbol{m}^{\pm}_{mn}$ and $\boldsymbol{n}^{\pm}_{mn}$ are solenoidal ($\operatorname{div}\boldsymbol{m}^{\pm}_{mn} = \operatorname{div}\boldsymbol{n}^{\pm}_{mn} = 0$) and are related by the expressions $\nabla\times\boldsymbol{m}^{\pm}_{mn} = k\boldsymbol{n}^{\pm}_{mn}$ и $\nabla\times\boldsymbol{n}^{\pm}_{mn} = k\boldsymbol{m}^{\pm}_{mn}$.

The general form of the expansion of an arbitrary vector field $\boldsymbol{F}$ in vector spherical functions is described by the expression

$$\boldsymbol{F}(r,\theta,\varphi) = \sum_\eta(\alpha_\eta\boldsymbol{m}_\eta + \beta_\eta\boldsymbol{n}_\eta + \delta_\eta\boldsymbol{l}_\eta), \tag{A1.2}$$

where η is the combined index of the vector spherical modes. Because the spherical vector functions are mutually orthogonal, the expansion coefficients are determined by the expressions

$$\alpha_\eta = \frac{\int r^2\mathrm{d}r\int_0^\pi\sin\theta\,\mathrm{d}\theta\int_0^{2\pi}\mathrm{d}\varphi(F_r m_{\eta r}+F_\theta m_{\eta\theta}+F_\varphi m_{\eta\varphi})}{\int\boldsymbol{m}_\eta\boldsymbol{m}_\eta^* r^2\mathrm{d}r\int_0^\pi\sin\theta\,\mathrm{d}\theta\int_0^{2\pi}\mathrm{d}\varphi}, \tag{A1.3}$$

$$\beta_\eta = \frac{\int r^2\mathrm{d}r\int\pi_0\sin\theta\,\mathrm{d}\theta\int_0^{2\pi}\mathrm{d}\varphi(F_r n_{\eta r}+F_\theta n_{\eta\theta}+F_\varphi n_{\eta\varphi})}{\int\boldsymbol{n}_\eta\boldsymbol{n}_\eta^* r^2\mathrm{d}r\int_0^\pi\sin\theta\,\mathrm{d}\theta\int_0^{2\pi}\mathrm{d}\varphi}, \tag{A1.4}$$

$$\delta_\eta = \frac{\int r^2 \mathrm{d}r \int_0^\pi \sin\theta\,\mathrm{d}\theta \int_0^{2\pi} \mathrm{d}\varphi (F_r l_{\eta r} + F_\theta l_{\eta\theta} + F_\varphi l_{\eta\varphi})}{\int \boldsymbol{l}_\eta \boldsymbol{l}_\eta^* r^2 \mathrm{d}r \int_0^\pi \sin\theta\,\mathrm{d}\theta \int_0^{2\pi} \mathrm{d}\varphi}. \quad \text{(A1.5)}$$

The integration over the radial coordinate should be performed within the orthogonality interval of the radial functions. The angular integrals entering the denominators in expressions A(1.3), (A1.4), and (A1.5), have the form (see, for example, [4])

$$\int_0^\pi \boldsymbol{m}_\eta \boldsymbol{m}_\eta^* \sin\theta\,\mathrm{d}\theta \int_0^{2\pi} \mathrm{d}\varphi = 2\pi(1+\delta_{0m}) \frac{n(n+1)}{(2n+1)} \frac{(n+m)!}{(n-m)!} \frac{Z_\nu^2(kr)}{kr}, \quad \text{(A1.6)}$$

$$\int_0^\pi \boldsymbol{n}_\eta \boldsymbol{n}_\eta^* \sin\theta\,\mathrm{d}\theta \int_0^{2\pi} \mathrm{d}\varphi = 2\pi(1+\delta_{0m}) \frac{n(n+1)}{(2n+1)} \frac{(n+m)!}{(n-m)!} \times \left[\frac{n+1}{2n+1} \frac{Z_{\nu-1}^2(kr)}{kr} + \frac{n}{2n+1} \frac{Z_{\nu+1}^2(kr)}{kr} \right], \quad \text{(A1.7)}$$

$$\int_0^\pi \boldsymbol{l}_\eta \boldsymbol{l}_\eta^* \sin\theta\,\mathrm{d}\theta \int_0^{2\pi} \mathrm{d}\varphi = 2\pi(1+\delta_{0m}) \frac{k^2}{(2n+1)} \frac{(n+m)!}{(n-m)!} \times \left[\frac{n}{2n+1} \frac{Z_{\nu-1}^2(kr)}{kr} + \frac{n+1}{2n+1} \frac{Z_{\nu+1}^2(kr)}{kr} \right], \quad \text{(A1.8)}$$

where δ_{0m} is the Kronecker delta.

Appendix 2. Useful formulas

Here, the formulas are presented, which are useful in the study of WGMs and were taken from handbook [26].

The coefficients of expansion of a near-surface wave in the spherical waves were calculated using the expression

$$\exp(\mathrm{i}x\cos\varphi) = \sum_{m=-\infty}^{\infty} \mathrm{i}^m J_m(x) \exp(\mathrm{i}m\varphi). \quad \text{(A2.1)}$$

The expressions

$$\frac{\mathrm{d}}{\mathrm{d}x} Z_\nu(x) = \frac{1}{2}[Z_{\nu-1}(x) - Z_{\nu+1}(x)], \quad \text{(A2.2)}$$

$$Z_\nu(x) = \frac{x}{2\nu}[Z_{\nu-1}(x) + Z_{\nu+1}(x)]. \quad \text{(A2.3)}$$

are useful for performing some transformations.

Expression (A2.3) is a recurrent relation and makes it possible to calculate functions with the next index, knowing two functions with previous indices. For this reason, expressions

$$J_{1/2}(x) = \left(\frac{2}{\pi x}\right)^{1/2} \sin x,\ J_{-1/2}(x) = \left(\frac{2}{\pi x}\right)^{1/2} \cos x. \quad \text{(A2.4)}$$

are important for calculating the Bessel functions with half-integer indices.

$$\int x Z_\nu^2(\alpha x)\mathrm{d}x = \frac{x^2}{2}\left[Z_\nu^2(\alpha x) - Z_{\nu-1}(\alpha x) Z_{\nu+1}(\alpha x)\right], \quad \text{(A2.5)}$$

and

$$\int_0^1 x^{\nu+1}(1-x^2)^\mu J_\nu(zx)\mathrm{d}x = \frac{2^\mu}{z^{\mu+1}} \Gamma(\mu+1) J_{\nu+\mu+1}(z), \quad \text{(A2.6)}$$

(where Γ is the Euler gamma function) were used in calculations involving Bessel functions. It follows from (A2.6) that

$$\int_0^\pi \sin^{\nu+1}\theta \cos^\mu\theta\, J_\nu(z\sin\theta)\mathrm{d}\theta = \begin{cases} 0 \text{ при } \mu = 2n+1, \\ 2\dfrac{2^\mu}{z^{\mu+1}} \Gamma(\mu+1) J_{\nu+\mu+1}(z) \text{ при } \mu = 2n, \end{cases} \quad \text{(A2.7)}$$

$$\Gamma\left(n+\frac{1}{2}\right) = \frac{\sqrt{\pi}}{2^n}(2n-1)!!, \quad \text{(A2.8)}$$

$$\Gamma\left(\frac{1}{2}\right) = \sqrt{\pi},\ \Gamma\left(-\frac{1}{2}\right) = -2\sqrt{\pi}, \quad \text{(A2.9)}$$

$$\Gamma(1) = \Gamma(2) = 1. \quad \text{(A2.10)}$$

The famous Stirling formula

$$n! \approx \left(\frac{n}{\mathrm{e}}\right)^n (2\pi n)^{1/2} \left(1 + \frac{1}{12n} + \frac{1}{288n} + \ldots\right). \quad \text{(A2.11)}$$

is used for calculating factorials of large numbers.

The adjoint Legendre polynomials for $m = n$ are described by a simple expression

$$P_n^n(\cos\theta) = (-1)^n (2n-1)!! \sin^n\theta. \quad \text{(A2.12)}$$

Other adjoint Legendre polynomials with large indices n and a small difference $n-m$ can be calculated using the relation

$$\frac{P_n^m(\theta)}{P_n^m(0)} \approx \frac{H_{n-m}(\sqrt{m}\,\theta)}{H_{n-m}(0)} \exp(-m\theta^2/2). \quad \text{(A2.13)}$$

References

1. Strutt J. (Lord Rayleigh) *Teoriya zvuka* (Theory of Sound) (Moscow: Gostekhizdat, 1955) Vol. 2.
2. Mie G. *Ann. Physik*, **25**, 377 (1908).
3. Debye P. *Ann. Physik*, **30**, 57 (1909).
4. Stratton J.A. *Electromagnetic Theory* (New York: McGraw-Hill, 1941; Moscow: OGIZ-Gostekhizdat, 1948).
5. Snyder A., Love J. *Optical Waveguide Theory* (London, New York: Chapman and Hall; Moscow: Radio i Svyaz', 1987).
6. Vainshtein L.A. *Elektromagnitnye volny* (Electromagnetic Waves) (Moscow: Sovetskoe Radio, 1957).
7. Gorodetsky M.L., Ilchenko V.S. *Opt. Commun.*, **113**, 133 (1994).
8. Knight J.C., Dubreuil N., Sandoghdar V., Hare J., Lefevre-Seguin V., Raimond J.M., Haroche S. *Opt. Lett.*, **20**, 1515 (1995).
9. Fock V.A. *Tablitsy funktsii Eiri* (Tables of Airy Functions) (Moscow: Izd. Research Institute-108, 1946).
10. Vainshtein L.A. *Otkrytye rezonatory i otkrytye volnovody* (Open Resonators and Open Waveguides) (Moscow: Sovetskoe Radio, 1966).
11. Lam C.C., Leung P.T., Young K. *J. Opt. Soc. Am. B*, **9**, 1585 (1992).

12. Shiller S. *Appl. Opt*., **32**, 2181 (1993).
13. Schiller S., Byer R.L. *Opt. Lett*., **16**, 1138 (1991).
14. Landau L.D., Lifshits E.M. *Kvantovaya mekhanika* (Quantum Mechanics) (Moscow: Nauka, 1984).
15. Rezac J.P., Rosenberger A.T. *Opt. Express*, **8**, 605 (2001).
16. Rezac J.P., Rosenberger A.T. *Proc. SPIE Int. Soc. Opt. Eng*., **4270**, 112 (2001).
17. Ilchenko V.S., Gorodetsky M.L., Vyatchanin S.P. *Opt. Commun*., **107**, 41 (1994).
18. Ishikava H., Tamaru H., Miyano K. *J. Opt. Soc. Am. A*, **17**, 802 (2000).
19. Lai H.M., Leung P.T., Yong K., Barber P.W., Hill S.C. *Phys. Rev. A*, **41**, 5187 (1990).
20. Weiss D.S., Sandoghdar V., Hare J., Lefevre-Seguin V., Raimond J.-M., Haroshe S. *Opt. Lett*., **20**, 1835 (1995).
21. Landau L.D., Lifshits E.M. *Elektrodinamika sploshnykh sred* (Electrodynamics of Continuous Media) (Moscow: Nauka, 1957).
22. Gorodetsky M.L., Savchenkov A.A., Ilchenko V.S. *Opt. Lett*., **21**, 453 (1996).
23. Vernooy D.W., Ilchenko V.S., Mabuchi H., Streed E.W., Kimbl H.J. *Opt. Lett*., **23**, 247 (1998).
24. Braginskii V.B., Il'chenko V.S. *Dokl. Akad. Nauk SSSR,* **32**, 307 (1987).
25. Tien P.K. *Appl. Opt*., **10**, 2395 (1970).
26. Gradshteyn I.S., Ryzhik I.M. *Table of Integrals, Series, and Products* (New York: Academic Press, 1980; Moscow: Nauka, 1971).
27. Zhang J.-Z., Leach D.H., Chang R.K. *Opt. Lett*., **13**, 270 (1988).
28. Barton J.P., Alexander D.R., Schaub S.A. *J. Appl. Phys*., **64**, 1632 (1988).
29. Gouesbet G., Grehan G. *J. Opt. Soc. Am. A*, **5**, 1427 (1988).
30. Lui C., Kaiser T., Lange S., Schweiger G. *Opt. Commun*., **117**, 521 (1995).
31. Dubreuil N., Knight J.C., Leventhal D.K., Sandoghdar V., Hare J., Lefevre V. *Opt. Lett*., **20**, 813 (1995).
32. Serpengüzel A., Arnold A., Griffel G., Lock J.A. *J. Opt. Soc. Am. B*, **14**, 790 (1997).
33. Lock J.A. *J. Opt. Soc. Am. A*, **15**, 2986 (1998).
34. Zvyagin A.V., Goto K. *J. Opt. Soc. Am. A*, **15**, 3003 (1998).
35. Gorodetsky M.L., Ilchenko V.S. *J. Opt. Soc. Am. B*, **16**, 147 (1999).
36. Ilchenko V.S., Yao X.S., Maleki L. *Opt. Lett*., **24**, 723 (1999).
37. Little B.E., Laine J.-P., Haus A. *J. Lightwave Technol*., **17**, 704 (1999).
38. Ishikawa H., Tamaru H., Miyano K. *J. Opt. Soc. Am. A*, **17**, 802 (2000).
39. Cai M., Painter O., Vahala K.J., Sercel P.C. *Opt. Lett*., **25**, 1430 (2000).
40. Xudong Fan, Phedon Palinginis, Scott Lacey, Haillin Wang. *Opt. Lett*., **25**, 1600 (2000).
41. Oraevsky A.N., Bandy D.K. *Opt. Commun*. (presented for publication).
42. Landau L.D., Lifshits E.M. *Teoriya polya* (Field Theory) (Moscow: Nauka, 1988).
43. Oraevsky A.N. *Usp. Fiz. Nauk,* **164**, 415 (1994).
44. Oraevsky A.N., Yarovitsky A.V, Velichansky V.L. *Kvantovaya Elektron.,* **31**, 897 (2001) [*Quantum Electron.,* **31**, 897 (2001)].
45. Baer T. *Opt. Lett*., **12**, 392 (1987).
46. Cai M., Painter O., Vahala K.J., Sercel P.C. *Opt. Lett*., **25**, 1430 (2000).
47. Sandoghdar V., Treussart F., Hare J., Lefevre-Seguin V., Raimond J.-M., Haroche S. *Phys. Rev. A*, **54**, R1777 (1996).
48. Oraevsky A.N., Scully M, Velichansky V.L. *Kvantovaya Elektron.* **25**, 211 (1998) [*Quantum Electron.,* **28**, 203 (1998)].
49. Oraevsky A.N., Scully M.O., Sakisyan T.V., Bandy D.K. *Laser Phys*., **9**, №5, 1 (1999).
50. Yamamoto Y., Pelton M. *Phys. Rev. A*, **59**, 2418 (1999).
51. Mu Yu., Savage C.M. *Phys. Rev. A*, **46**, 5944 (1992).
52. Loffler M., Meyer G.M., Walther H. *Phys. Rev. A*, **55**, 3923 (1997).
53. Kozlovsky A.V., Oraevsky A.N. *Zh. Eksp. Teor. Fiz.,* **115**, 1210 (1999).
54. Oraevsky A.N. *Usp. Fiz. Nauk,* **171**, 681 (2001); *Kvantovaya Elektron.,* **31**, 1038 (2001) [*Quantum Electron.,* **31**, 1038 (2001)].
55. McCall S.L., Levi A.F.J., Slusher R.E., Pearton S.J., Logan R.A. *Phys. Lett*., **60**, 289 (1992).
56. Levi A.F.J., Slusher R.E., McCall S.L., Tanbun-Ek T., Coblenz D.L., Pearton S.J. *Electron. Lett*., **28**, 101 (1992).
57. Levi A.F.J., Slusher R.E., McCall S.L., Glass J.L., Tanbun-Ek T., Pearton S.J. *Appl. Phys. Lett*., **62**, 561 (1993).
58. Eschmann A., Gardiner C.W. *Phys. Rev. A*, **49**, 2907 (1994).
59. Kurizki G., Nitzan A. *Phys. Rev. A*, **38**, 267 (1988).
60. Ledneva G.P., Astaf'eva L.G. *Opt. Spektrosk.,* **80**, 858 (1996).
61. Kotomtseva L.A., Lednyeva G.P., in *Diffractive Optics and Optical Microsystems* (New York: Plenum Press, 1997) p. 83.
62. Tzeng H.M., Wall K.F., Chang R.K. *Opt. Lett*., **9**, 499 (1984).
63. Taniguchi H., Tanosaki S. *Japan J. Appl. Phys*., **32**, L1615 (1993).
64. Datsyuk V.V., Izmailov I.A., Kochelap V.A., in *Kvantovaya Elektronika* (Kiev: Naukova Dumka, 1990) Vol. 38, p. 56.
65. Braginsky V.B., Gorodetsky M.L., Ilchenko V.S. *Phys. Lett*., **137**, 393 (1989).
66. Lin H.-B., Huston A.L., Eversole J.D., Campillo A.J. *Opt. Lett*., **11**, 614 (1986).
67. Kwok A.S., Chang R.K. *Opt. Lett*., **18**, 1597 (1993).
68. Chowdhury D.Q., Hill S.C., Mazumder Md.M. *IEEE J. Quantum Electron*., **29**, 2553 (1993).
69. Oraevsky A.N., Bandy D.K. *Kvantovaya Elektron.,* **22**, 211 (1995) [*Quantum Electron.,* **25**, 195 (1995)].
70. Velichansky V.L., Zibrov A.S., Kargopol'tsev V.S., Molochev V.I., Nikitin V.V., Sautenkov V.A., Kharisov G.G., Tyurikov D.A. *Pis'ma Zh. Tekh. Fiz.,* **4**, 1087 (1978).
71. Belenov E.M., Velichansky V.L., Zibrov A.S., Nikitin V.V., Sautenkov V.A., Uskov A.V. *Kvantovaya Elektron.,* **10**, 1232 (1983) [*Sov. J. Quantum Electron.,* **13**, 792 (1983)].
72. Vasil'ev V.V., Velichansky V.L., Gorodetsky M.L., Il'chenko V.S., Holberg L., Yarovitsky A.V. *Kvantovaya Elektron.,* **23**, 675 (1996) [*Quantum Electron.,* **26**, 657 (1996)].
73. Rezac J.P., Rosenberger A.T. *Proc. SPIE Int. Soc. Opt. Eng*., **4265**, 102 (2001).
74. Braginsky V.B., Vorontsov Y.L., Thorne K.S. *Science*, **209**, 547 (1980).
75. Brune M., Haroshe S., Lefevre V., Raimond J.M., Zagury N. *Phys. Rev. Lett*., **65**, 976 (1990).
76. Mabuchi H., Kimble H.J. *Opt. Lett*., **19**, 749 (1994).
77. Treussart F., Hare J., Collot V., Weiss D.S., Sandoghdar V., Raimond J.M., Haroche S. *Opt. Lett*., **19**, 1651 (1994).
78. Vernooy D.W., Furusava A., Georgiades N.Ph., Ilchenko V.S., Kimble H.J. *Phys. Rev. A*, **57**, R2293 (1998).
79. 79. Vinogradov A.V., Zorev N.N., Kozhevnikov I.N., Yakushkin I.G. *Zh. Eksp. Teor. Fiz.,* **89**, 2124 (1985).
80. Kozhevnikov I.N. *Trudy FIAN,* **196**, 143 (1989).
81. Ishimaru A. *Wave Propagation and Scattering in Random Media* (New York: Academic Press, 1978, Moscow: Mir,1981) Vols 1, 2.
82. Klimov V.V., Ducloy M, Letokhov V.S. *Kvantovaya Elektron.,* **31**, 569 (2001) [*Quantum Electron.,* **31**, 569 (2001)].
83. Frantsesson A.V., Zuev V.S. *J. Russian Laser Research*, **22**, 437 (2001).